Electronic Supplementary Material (ESI) for Physical Chemistry Chemical Physics.

Multiphoton breakdown of acetylene; Formation of organic building block fragments

Meng-Xu Jiang[1], Ioannis Giannakidis[2], Peter C. Samartzis[2]* and Ágúst Kvaran[1]*

1. *Science Institute, University of Iceland, Dunhagi 3, 107 Reykjavík, Iceland.*
2. *Institute of Electronic Structure and Laser, Foundation for Research and Technology-Hellas, Vassilika Vouton, 71110 Heraklion, Greece.*

Supplementary material

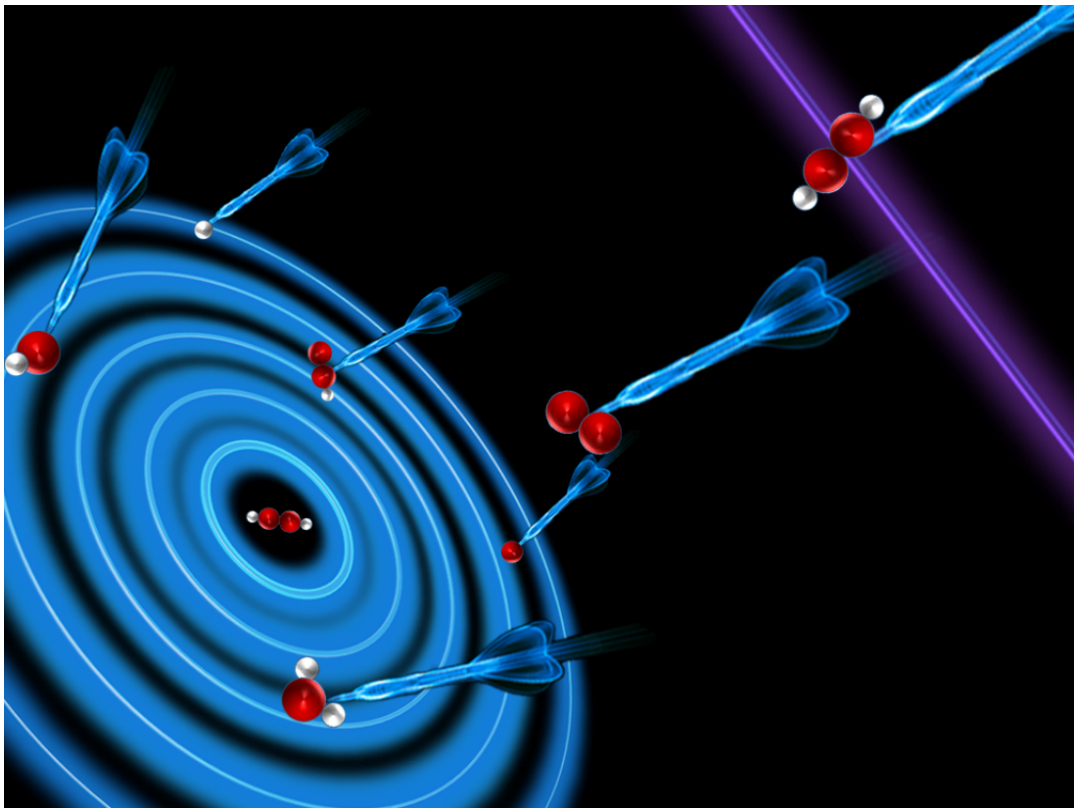

Content: **pages:**

Figures:

Content: **pages:**

Tables:

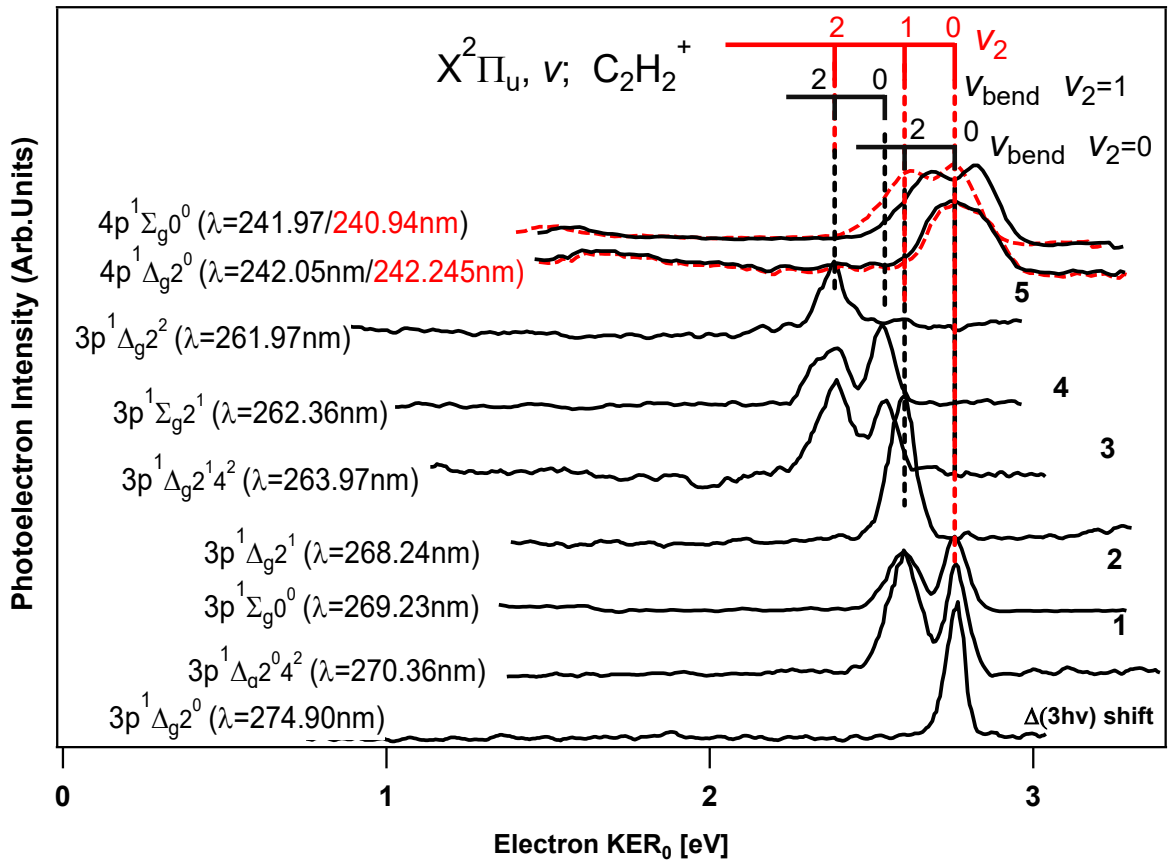

Fig. S1, Photoelectron spectra: Photoelectron spectra extracted from reference **[1]** (black) and from reference **[2]** (red) plotted as a function of the kinetic energy release (KER) for the spectrum derived by the λ = 261.97 nm excitation ("reference spectrum") shifted by three- photon energy differences, (Δ(3*hv*)) with respect to the "reference spectrum" (see main text / paper). Rydberg states and excitation wavelengths are indicated to the left. KER thresholds / assignments for ionization of fragments, according to reference **[1]** are indicated by sticks above the spectra.

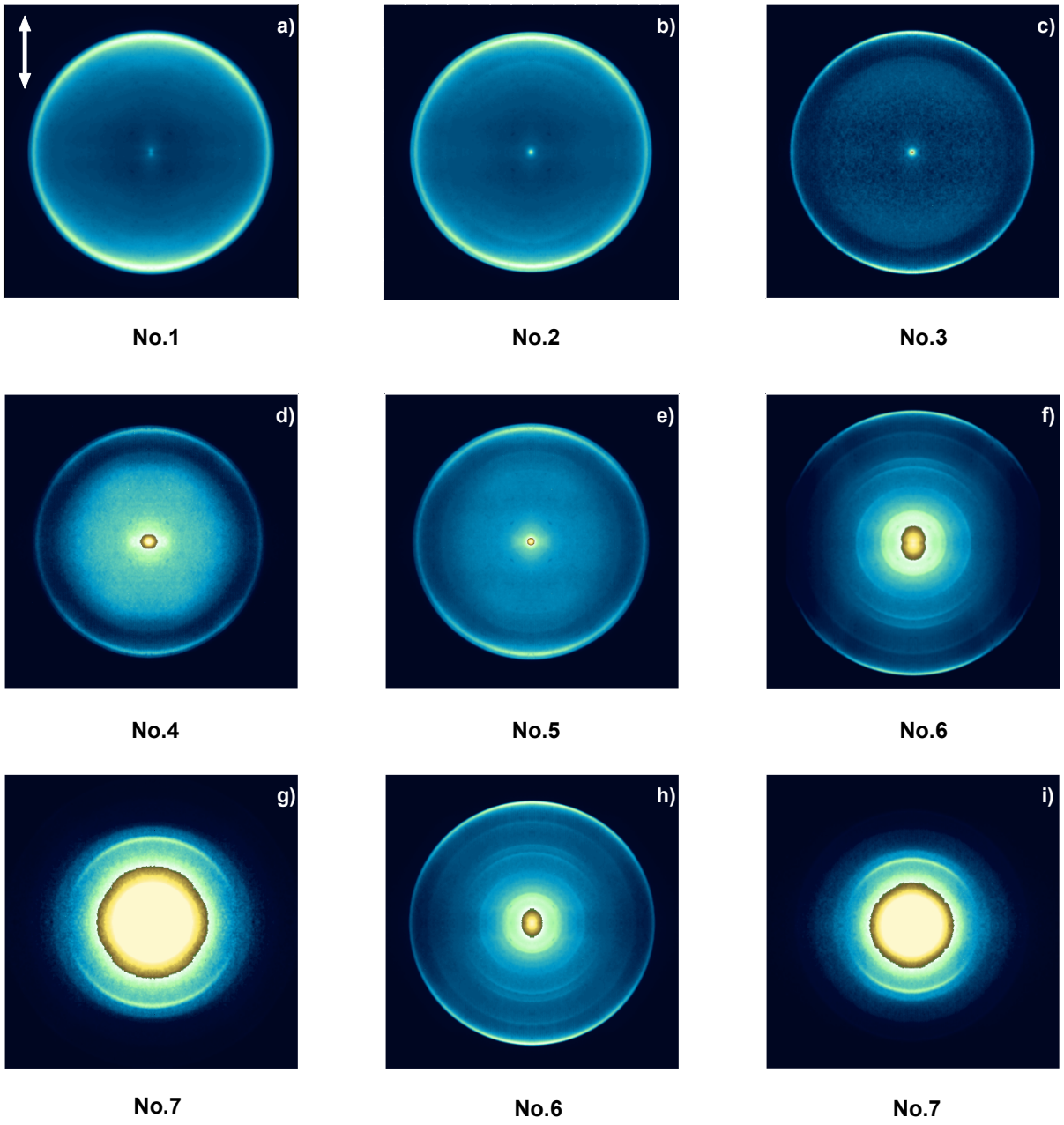

Fig. S2, photoelectron images: Photoelectron images for the excitations (no. 1 – 7) listed in **Table S1** (**Table 1** in paper). Images (a)-(g) and (h)-(i) were recorded for repeller voltages of -3kV and -5kV, respectively. The laser polarization is indicated by a double arrow in (a).

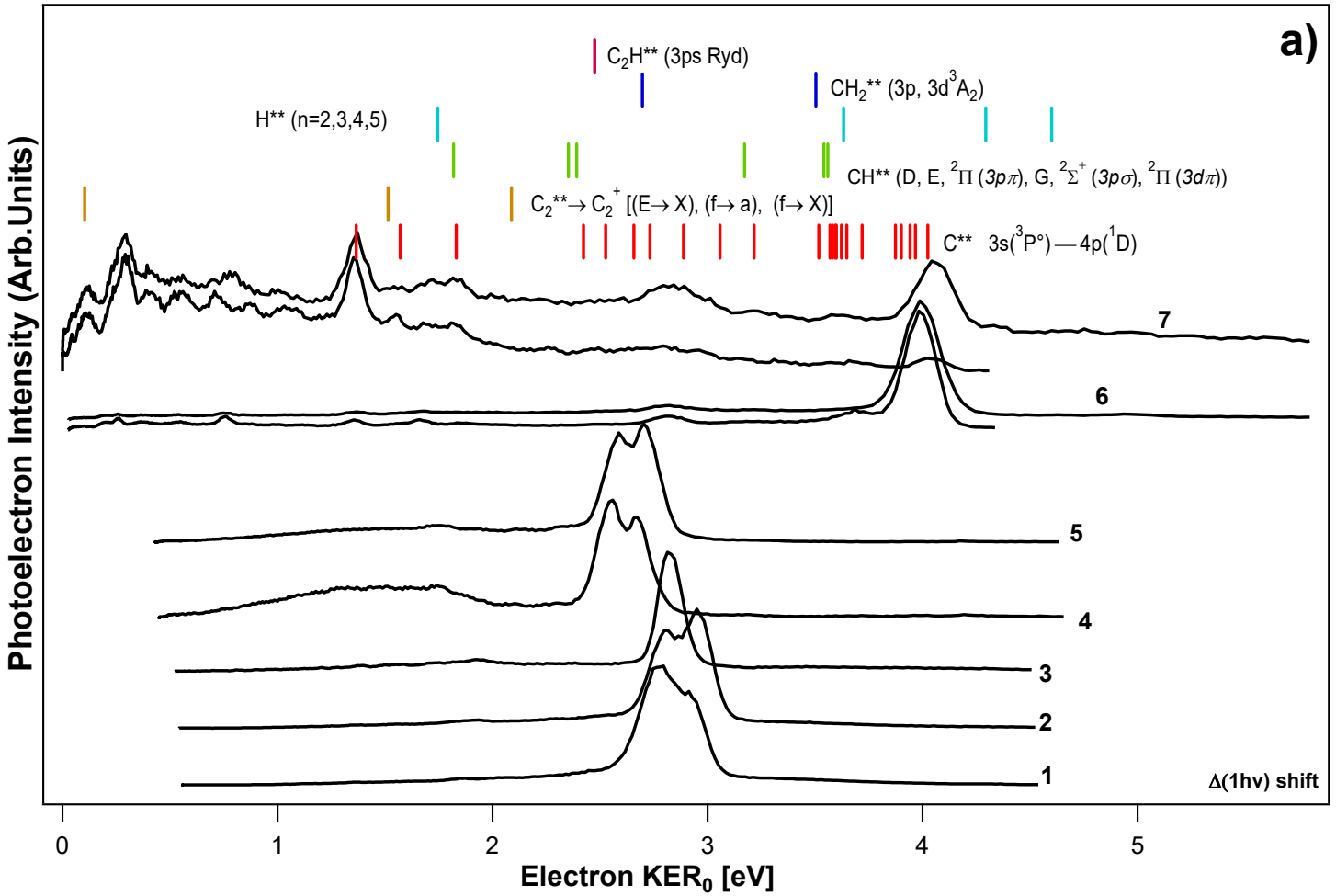

Fig. S3 (a), Electron KERs and energy thresholds: e-KERs derived from images no. 1 – 7 (**Table S1**) plotted as a function of the kinetic energy release (KER) for the no. 7 (KER_0), shifted by one-photon energy differences, ($\Delta(1h\nu)$) with respect to the "reference spectrum", no. 7 (see main text). KER thresholds for ionization of fragments, as specified, are indicated by sticks above the spectra.

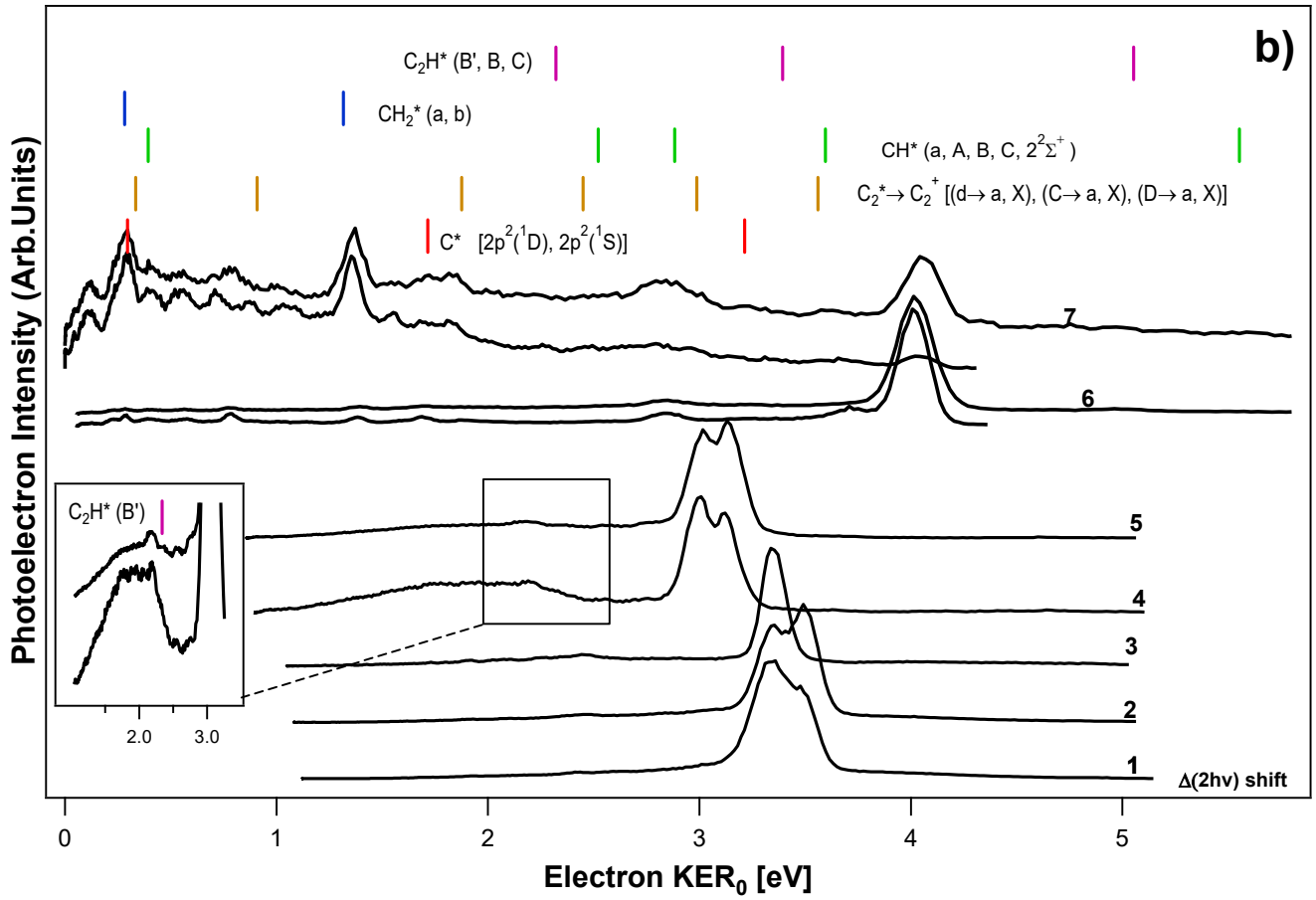

Fig. S3 (b), Electron KERs and energy thresholds: e-KERs derived from images no. 1 – 7 (**Table S1**) plotted as a function of the kinetic energy release (KER) for the no. 7 (KER_0), shifted by two-photon energy differences, ($\Delta(2h\nu)$) with respect to the "reference spectrum", no. 7 (see main text). KER thresholds for ionization of fragments, as specified, are indicated by sticks above the spectra.

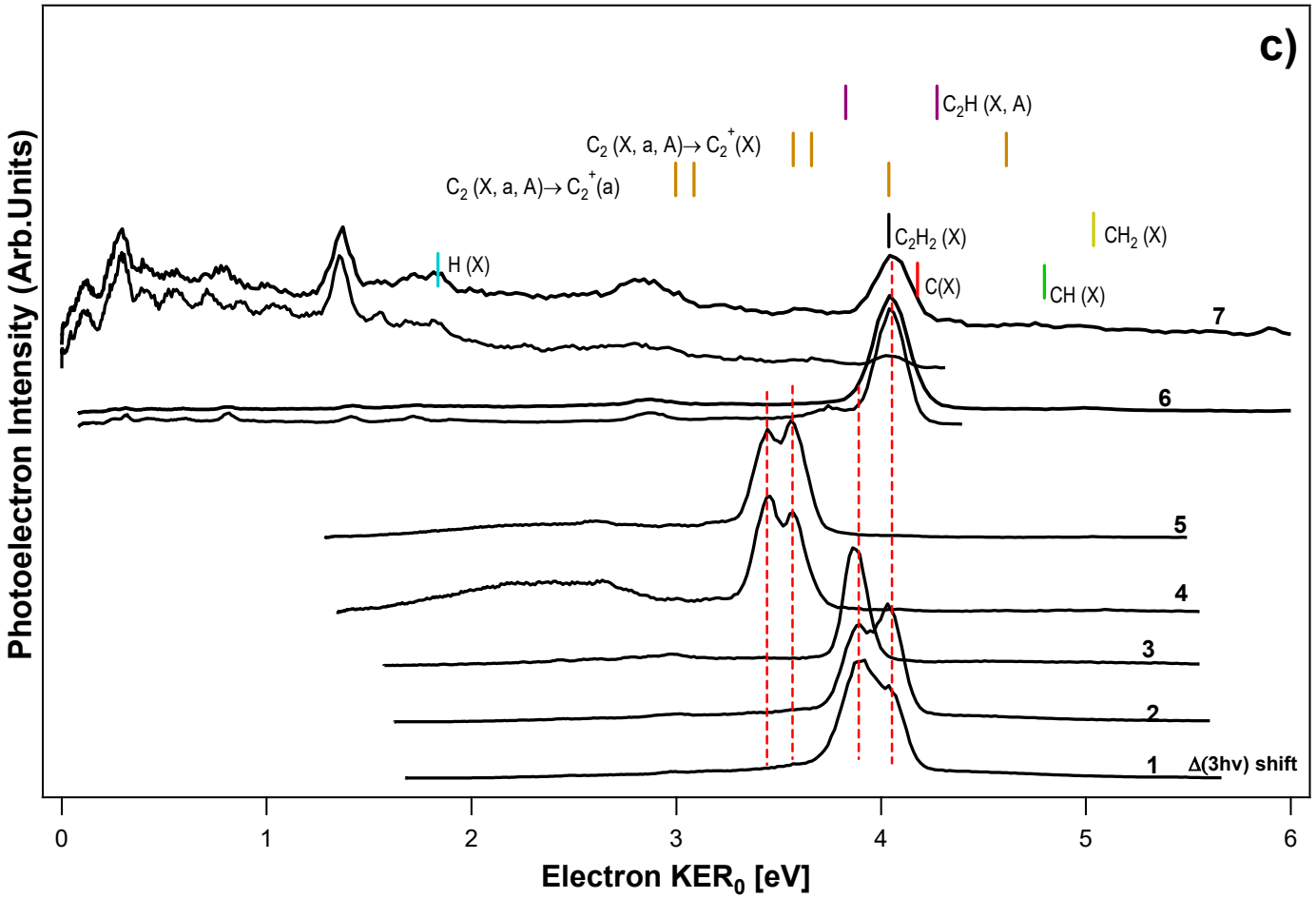

Fig. S3 (c), Electron KERs and energy thresholds: e-KERs derived from images no. 1 – 7 (**Table S1**) plotted as a function of the kinetic energy release (KER) for the no. 7 (KER_0), shifted by three-photon energy differences, ($\Delta(3h\nu)$) with respect to the "reference spectrum", no. 7 (see main text). KER thresholds for ionization of fragments, as specified, are indicated by sticks above the spectra.

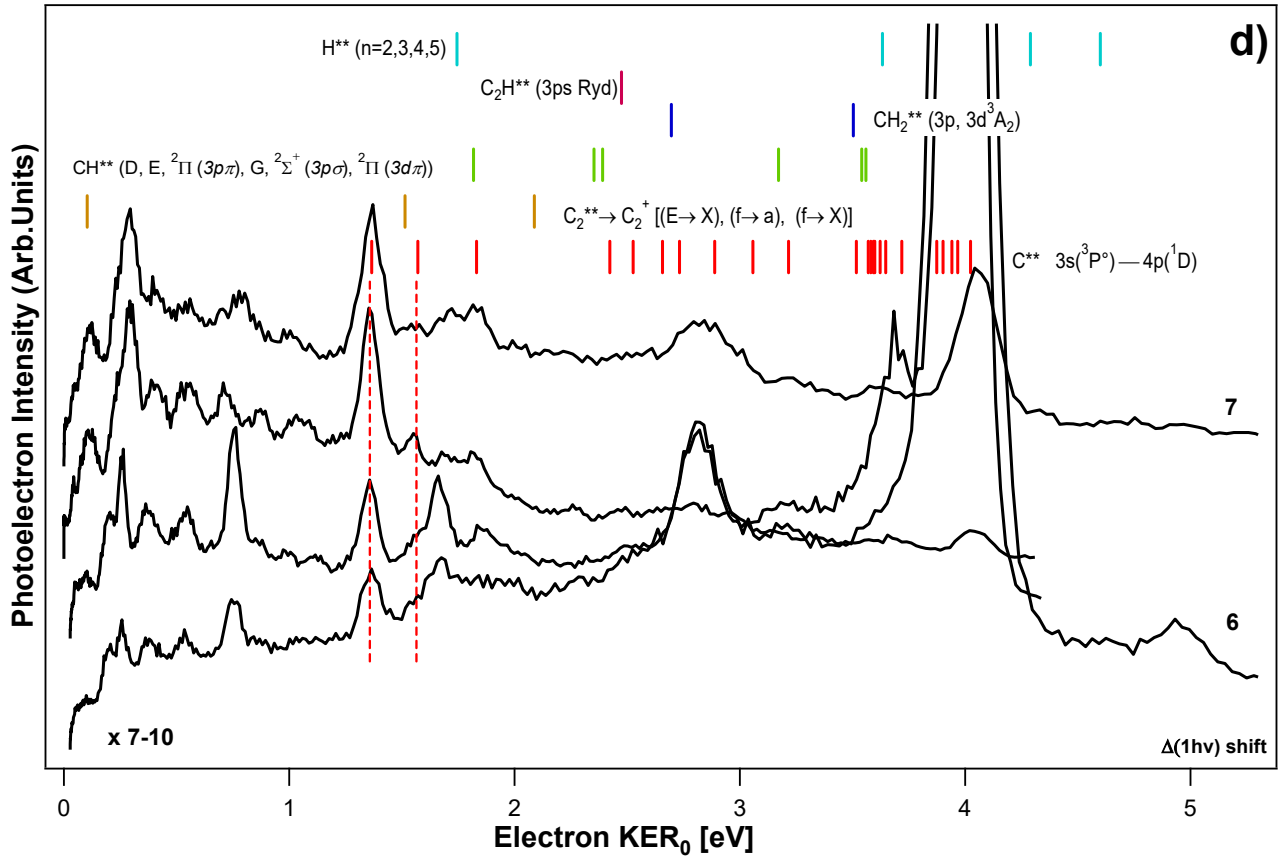

Fig. S3 (d), Electron KERs and energy thresholds: e-KERs derived from images no. 6-7 (**Table S1**) plotted as a function of the kinetic energy release (KER) for the no. 7 (KER_0), shifted by one-photon energy differences, ($\Delta(1h\nu)$) with respect to the "reference spectrum", no. 7 (see main text). KER thresholds for ionization of fragments, as specified, are indicated by sticks above the spectra. The spectrum for no.6 is magnified by factors 7-10.

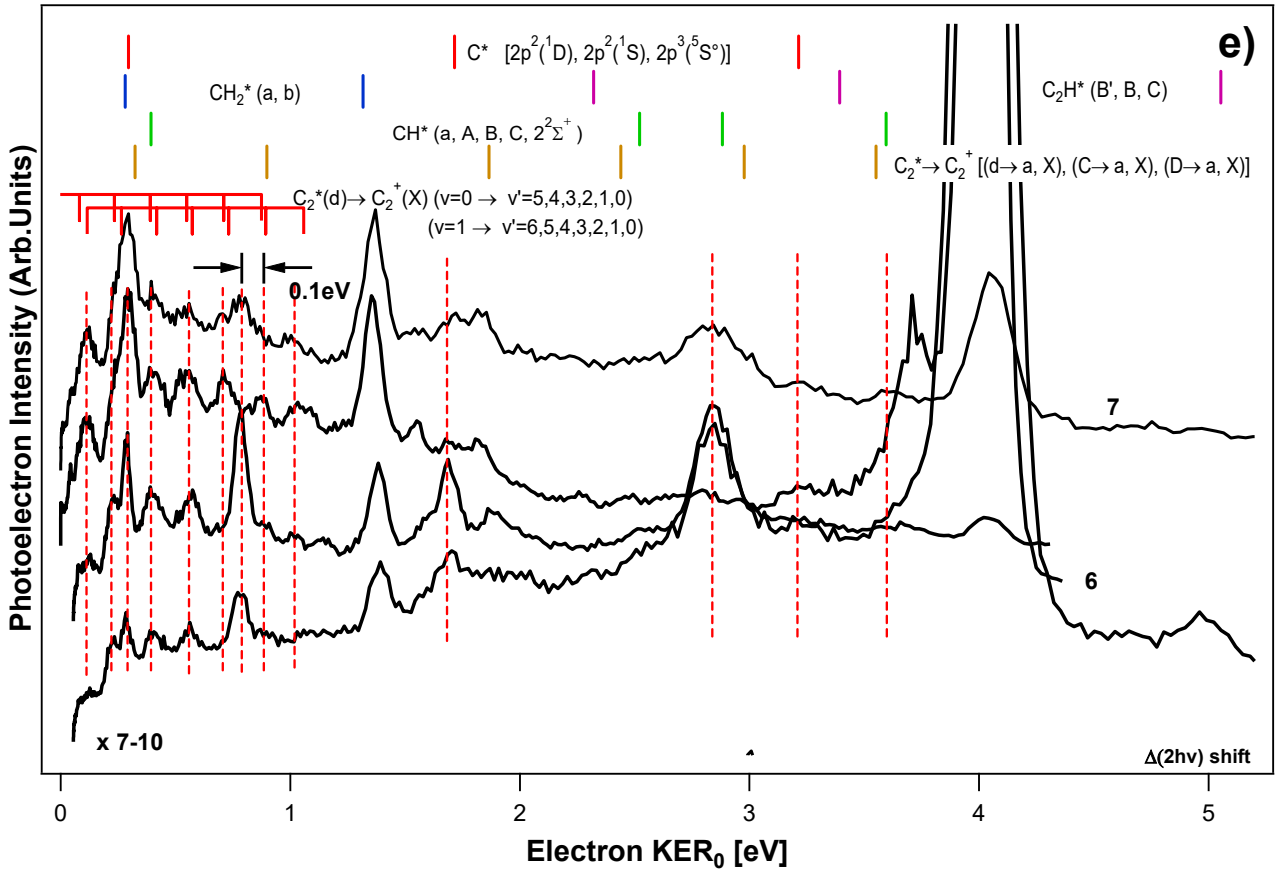

Fig. S3 (e), Electron KERs and energy thresholds: e-KERs derived from images no. 6-7 (**Table S1**) plotted as a function of the kinetic energy release (KER) for the no. 7 (KER_0), shifted by two-photon energy differences, ($\Delta(2h\nu)$) with respect to the "reference spectrum", no. 7 (see main text). KER thresholds for ionization of fragments, as specified, are indicated by sticks above the spectra. The spectrum for no.6 is magnified by factors 7-10.

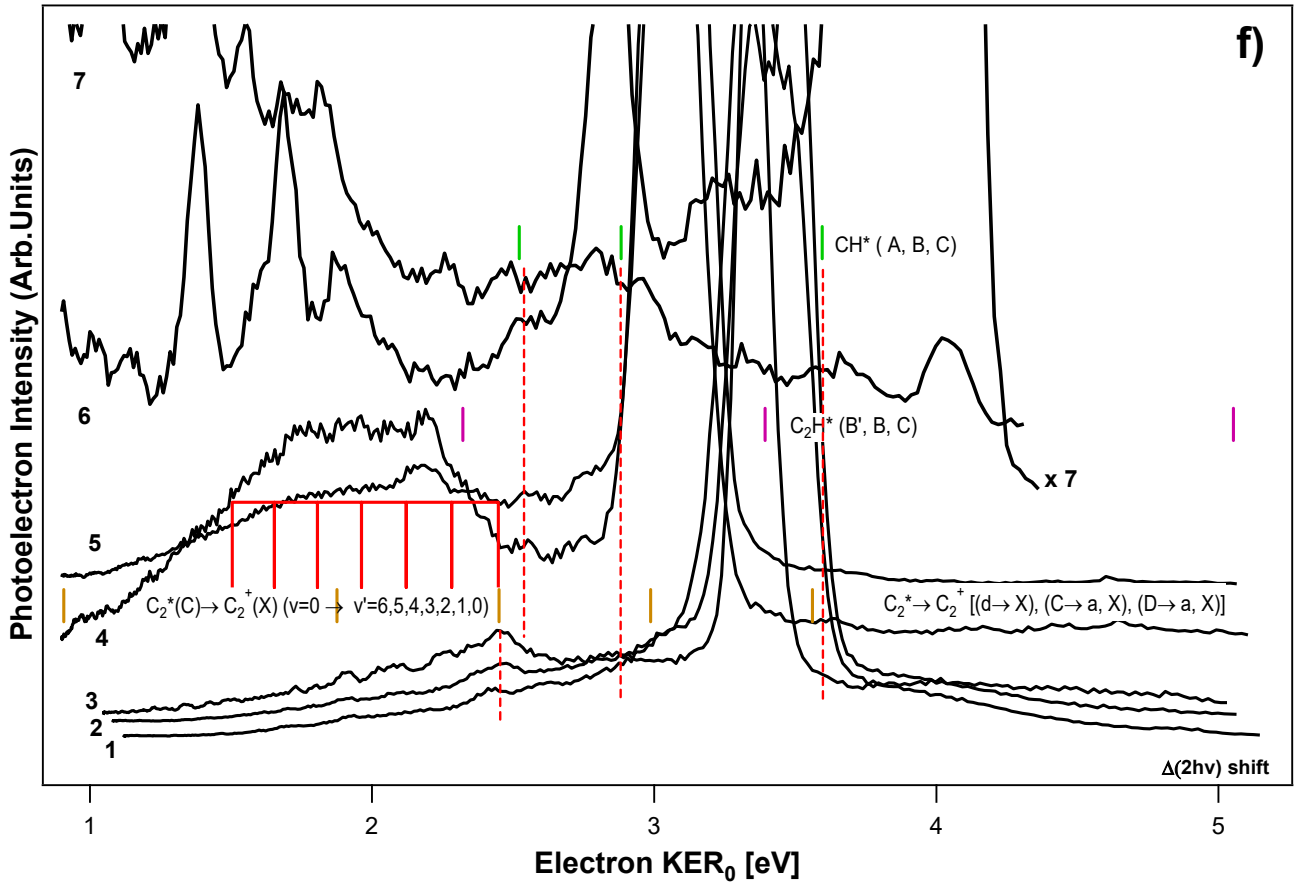

Fig. S3 (f), Electron KERs and energy thresholds: e-KERs derived from images no. 1-7 (**Table S1**) plotted as a function of the kinetic energy release (KER) for the no. 7 (KER_0), shifted by two-photon energy differences, ($\Delta(2h\nu)$) with respect to the "reference spectrum", no. 7 (see main text). KER thresholds for ionization of fragments, as specified, are indicated by sticks. The spectrum for no.1-5 is magnified.

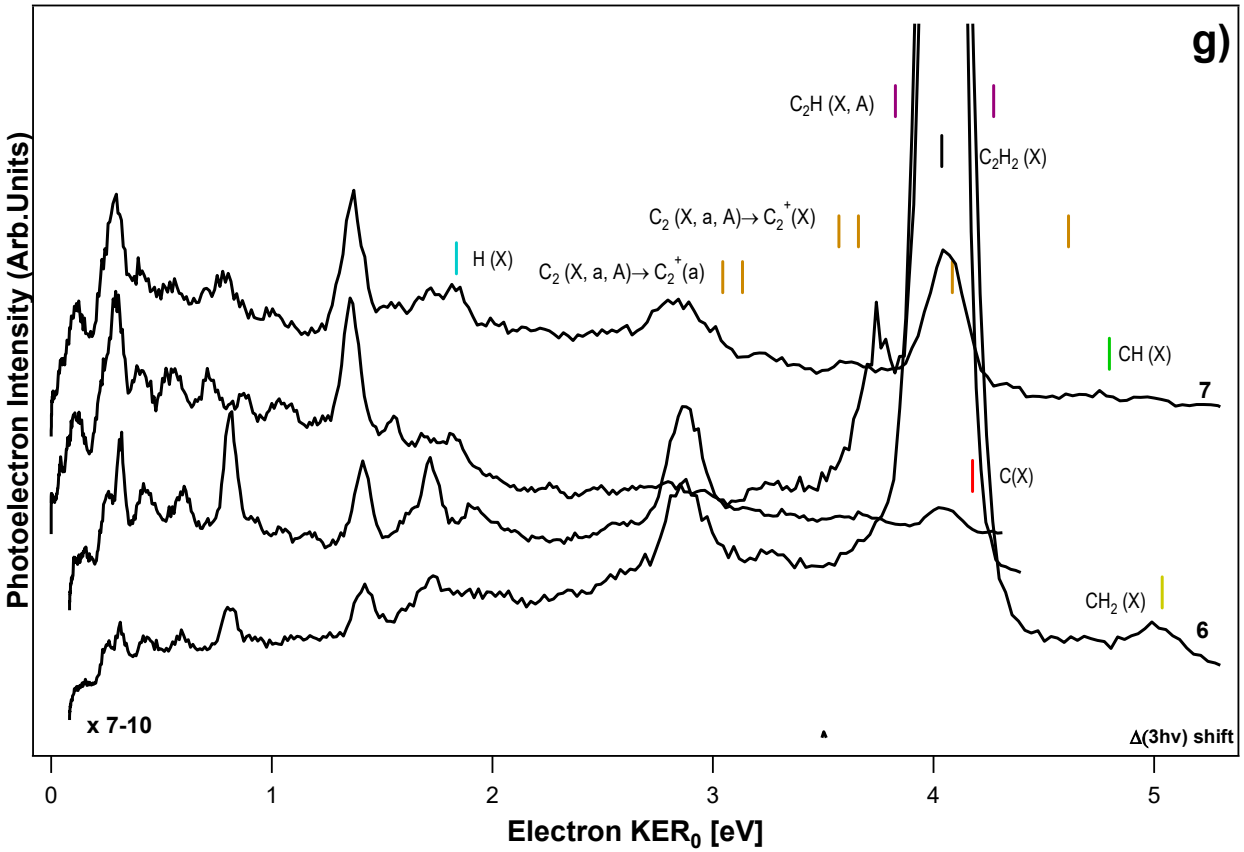

Fig. S3 (g), Electron KERs and energy thresholds: e-KERs derived from images no. 6-7 (**Table S1**) plotted as a function of the kinetic energy release (KER) for the no. 7 (KER_0), shifted by three-photon energy differences, ($\Delta(3h\nu)$) with respect to the "reference spectrum", no. 7 (see main text). KER thresholds for ionization of fragments, as specified, are indicated by sticks. The spectrum for no.6 is magnified as indicated.

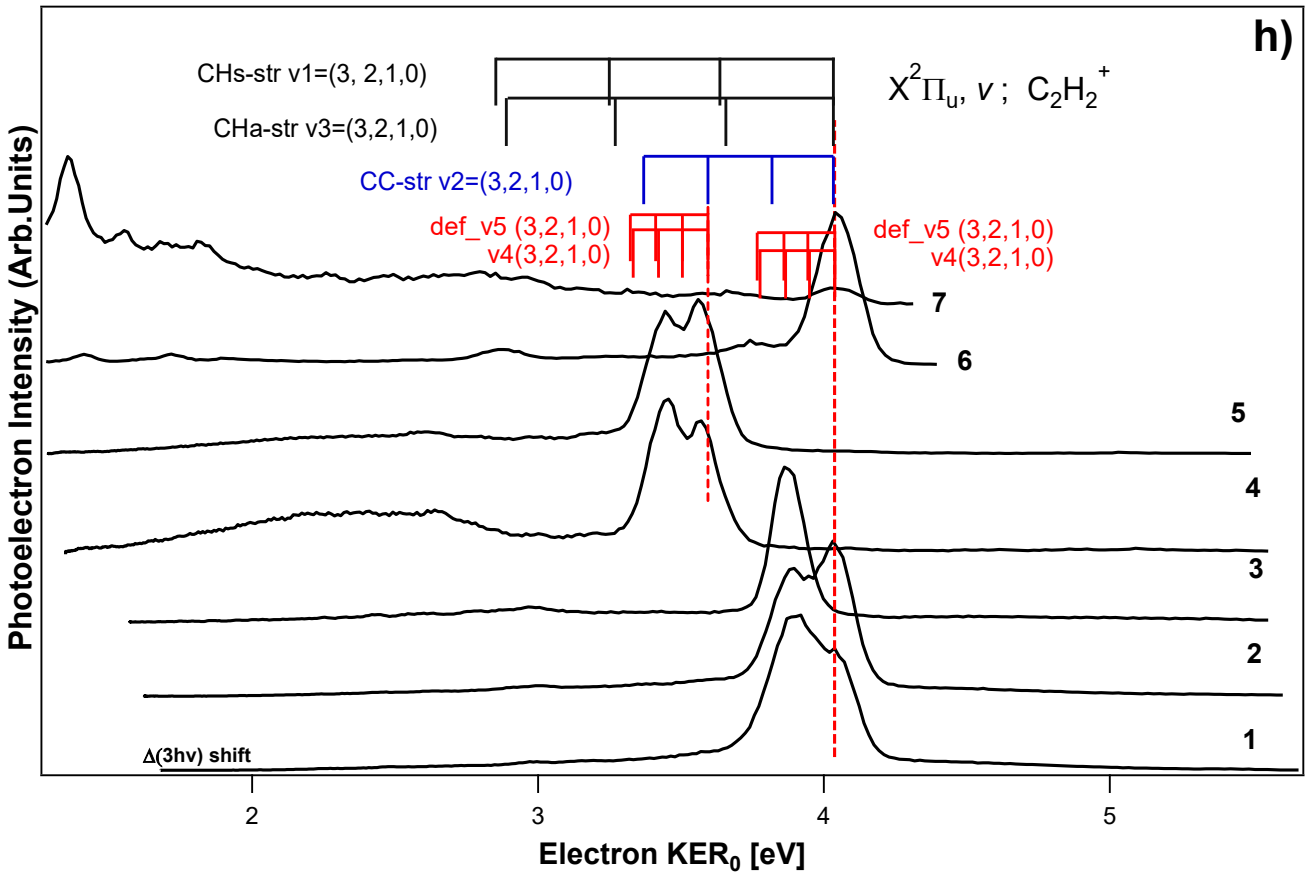

Fig. S3 (h), Electron KERs and energy thresholds: e-KERs derived from images no. 1-7 (**Table S1**) plotted as a function of the kinetic energy release (KER) for the no. 7 (KER_0), shifted by three-photon energy differences, ($\Delta(3h\nu)$) with respect to the "reference spectrum", no. 7 (see main text). KER thresholds for autoionization of superexcited C_2H_2, ($C_2H_2^{\#}$), as specified, are indicated by sticks above the spectra.

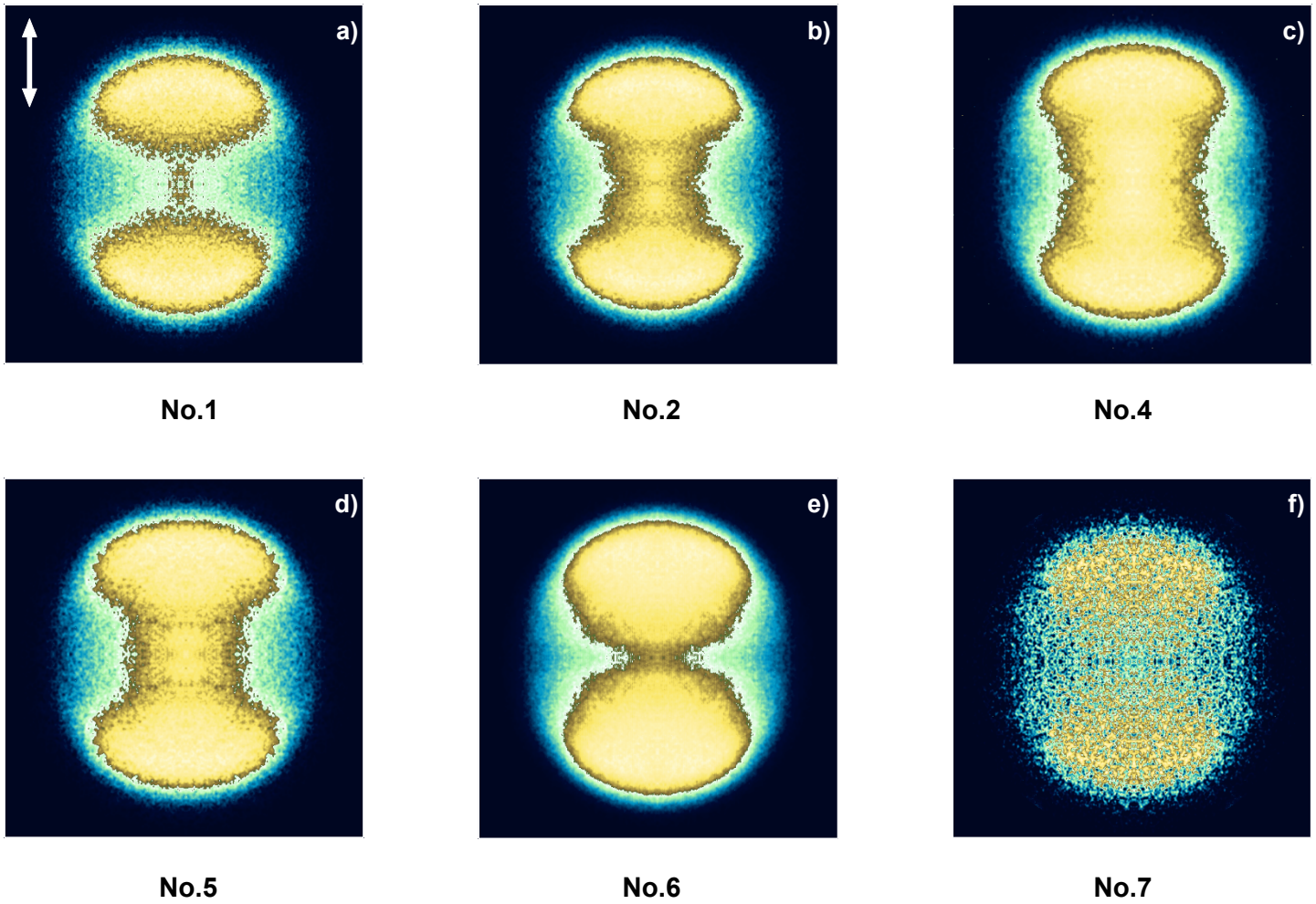

Fig. S4, H^+ ion images: Images recorded for the excitation no.1-2 and 4-7 as specified in **Table S1**. The laser polarization is indicated by a double arrow in (a).

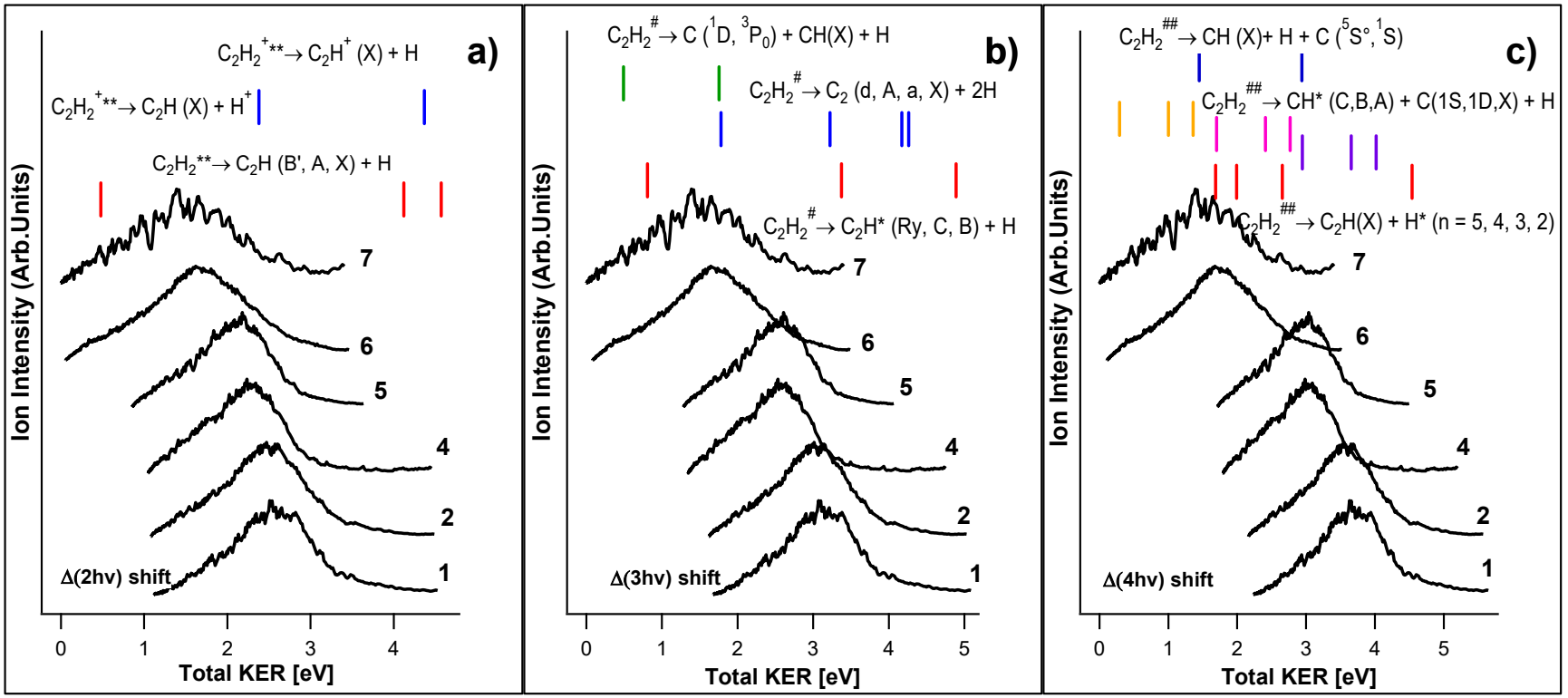

Fig. S5, H^+ kinetic energy release spectra (KERs): Ion kinetic energy release spectra (Ion-KERs) derived from the images no.1,2,4 - 7 (see **Table S1**). The spectra are plotted as a function of the total kinetic energy release for the no. 7 (Total KER_0) and shifted by n-photon energy differences (Δ(n*hv*)) with respect to the "reference spectrum", no. 7 (see main text) as, Δ(*2hv*) (a), Δ(*3hv*) (b) and Δ(*4hv*) (c). KER thresholds for fragment formations by n-photo-dissociation (n = 2, 3 and 4 for photodissociation or autoionization via the C_2H_2**, $C_2H_2^{\#}$ and $C_2H_2^{\#\#}$ intermediate species; see main text), as specified, are indicated by sticks above the spectra.

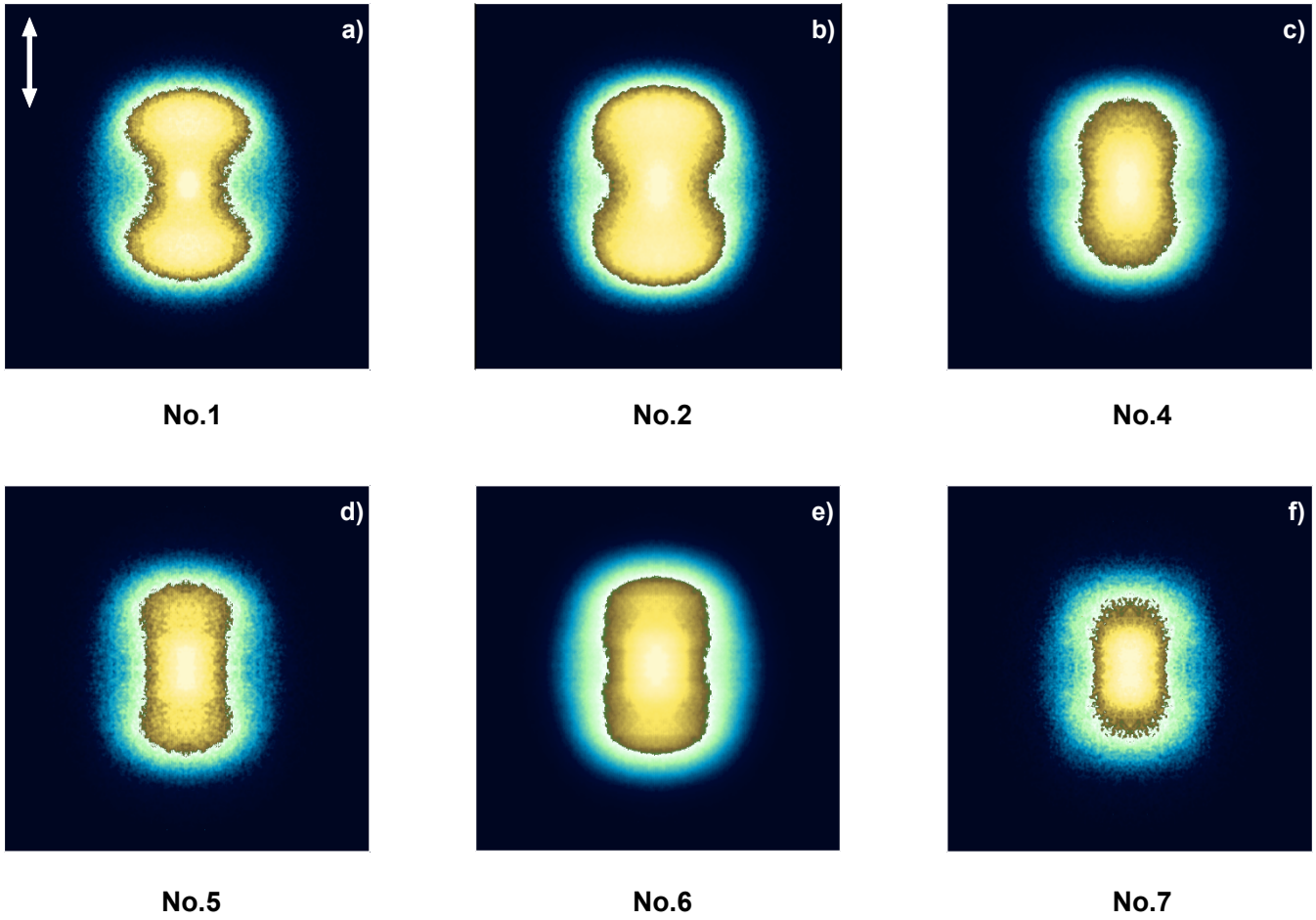

Fig. S6, C^+ ion images: Images recorded for the excitation no.1-2 and 4-7 as specified in **Table S1**. The laser polarization is indicated by a double arrow in (a).

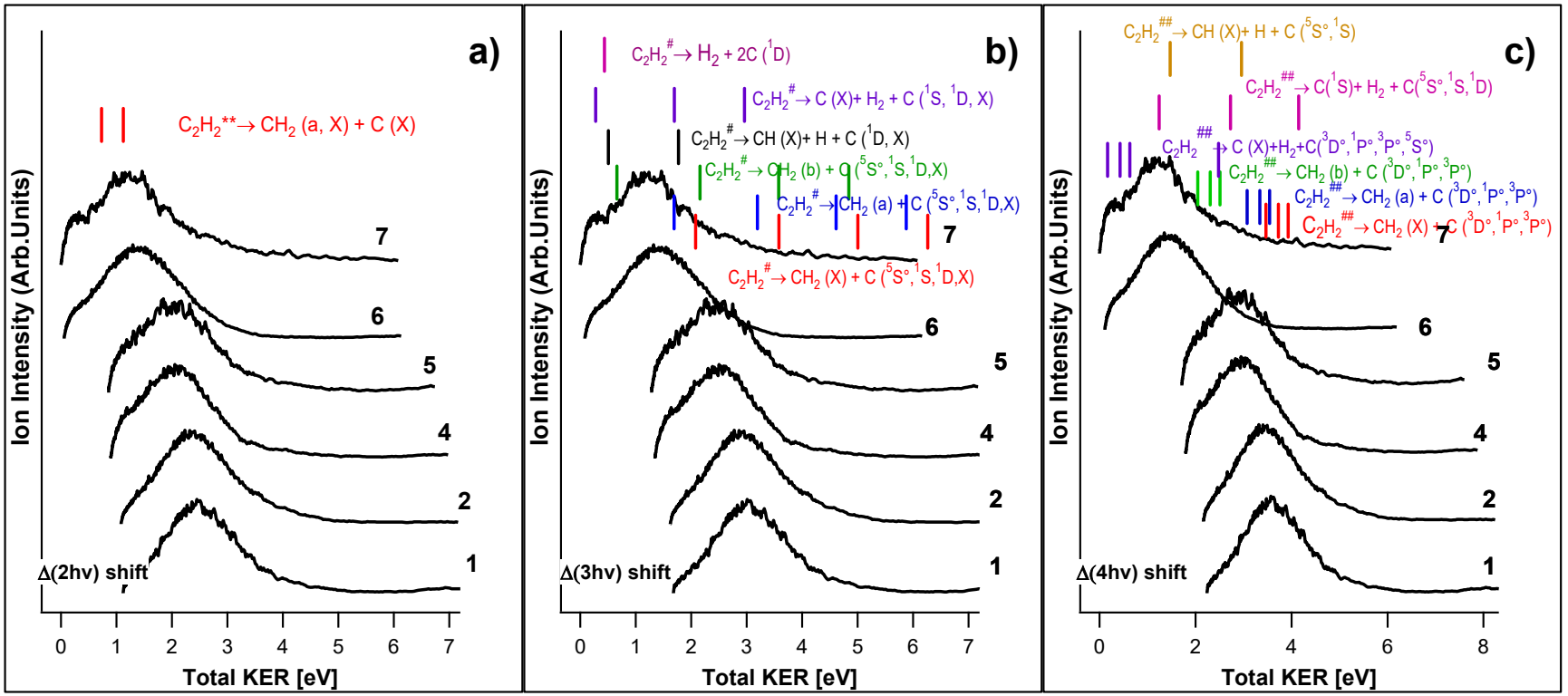

Fig. S7, C^+ kinetic energy release spectra (KERs): Ion kinetic energy release spectra (Ion-KERs) derived from the images no.1,2,4 - 7 (see **Table S1**). The spectra are plotted as a function of the total kinetic energy release for the no. 7 (Total KER_0) and shifted by n-photon energy differences (Δ(n*hv*)) with respect to the "reference spectrum", no. 7 (see main text) as, Δ(*2hv*) (a), Δ(*3hv*) (b) and Δ(*4hv*) (c). KER thresholds for fragment formations by n-photo-dissociation (n = 2, 3 and 4 for photodissociation via the C_2H_2**, $C_2H_2^{\#}$ and $C_2H_2^{\#\#}$ intermediate species; see main text), as specified, are indicated by sticks above the spectra.

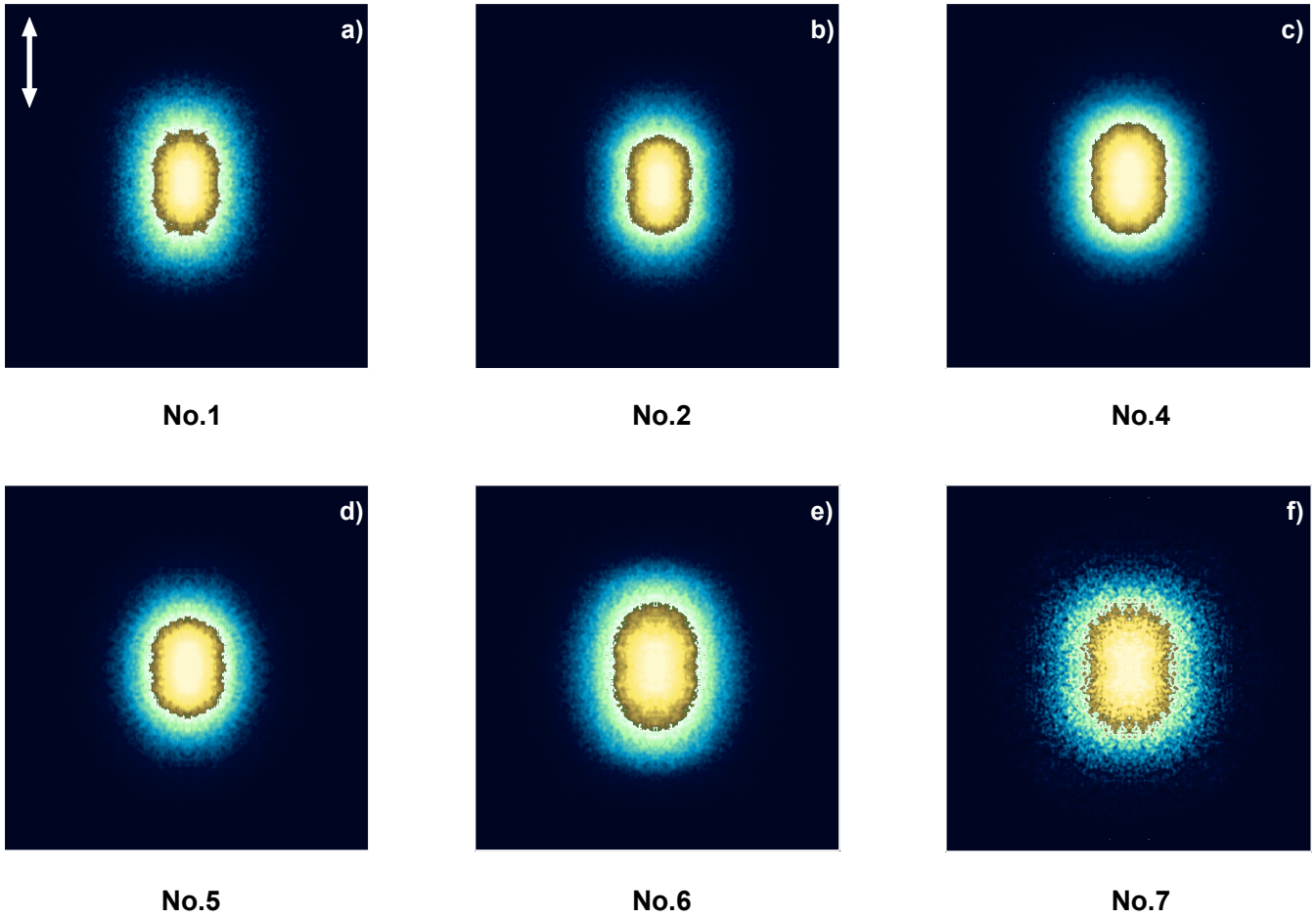

Fig. S8, CH^+ ion images: Images recorded for the excitation no.1-2 and 4-7 as specified in **Table S1**. The laser polarization is indicated by a double arrow in (a).

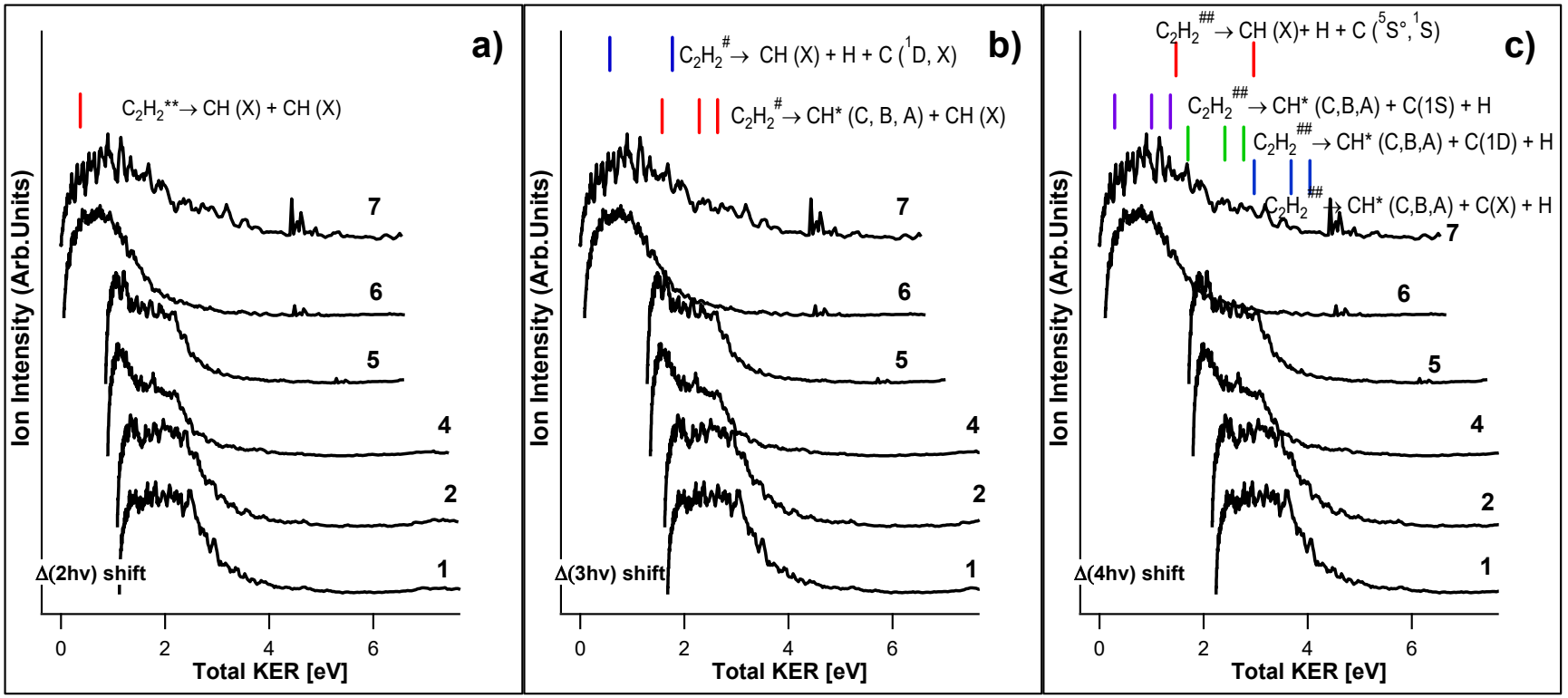

Fig. S9, CH^+ kinetic energy release spectra (KERs): Ion kinetic energy release spectra (Ion-KERs) derived from the images no.1,2,4 -7 (see **Table S1**). The spectra are plotted as a function of the total kinetic energy release for the no. 7 (Total KER_0) and shifted by n-photon energy differences (Δ(n*hv*)) with respect to the "reference spectrum", no. 7 (see main text) as, Δ(*2hv*) (a), Δ(*3hv*) (b) and Δ(*4hv*) (c). KER thresholds for fragment formations by n-photo-dissociation (n = 2, 3 and 4 for photodissociation via the C_2H_2**, $C_2H_2^{\#}$ and $C_2H_2^{\#\#}$ intermediate species; see main text), as specified, are indicated by sticks above the spectra.

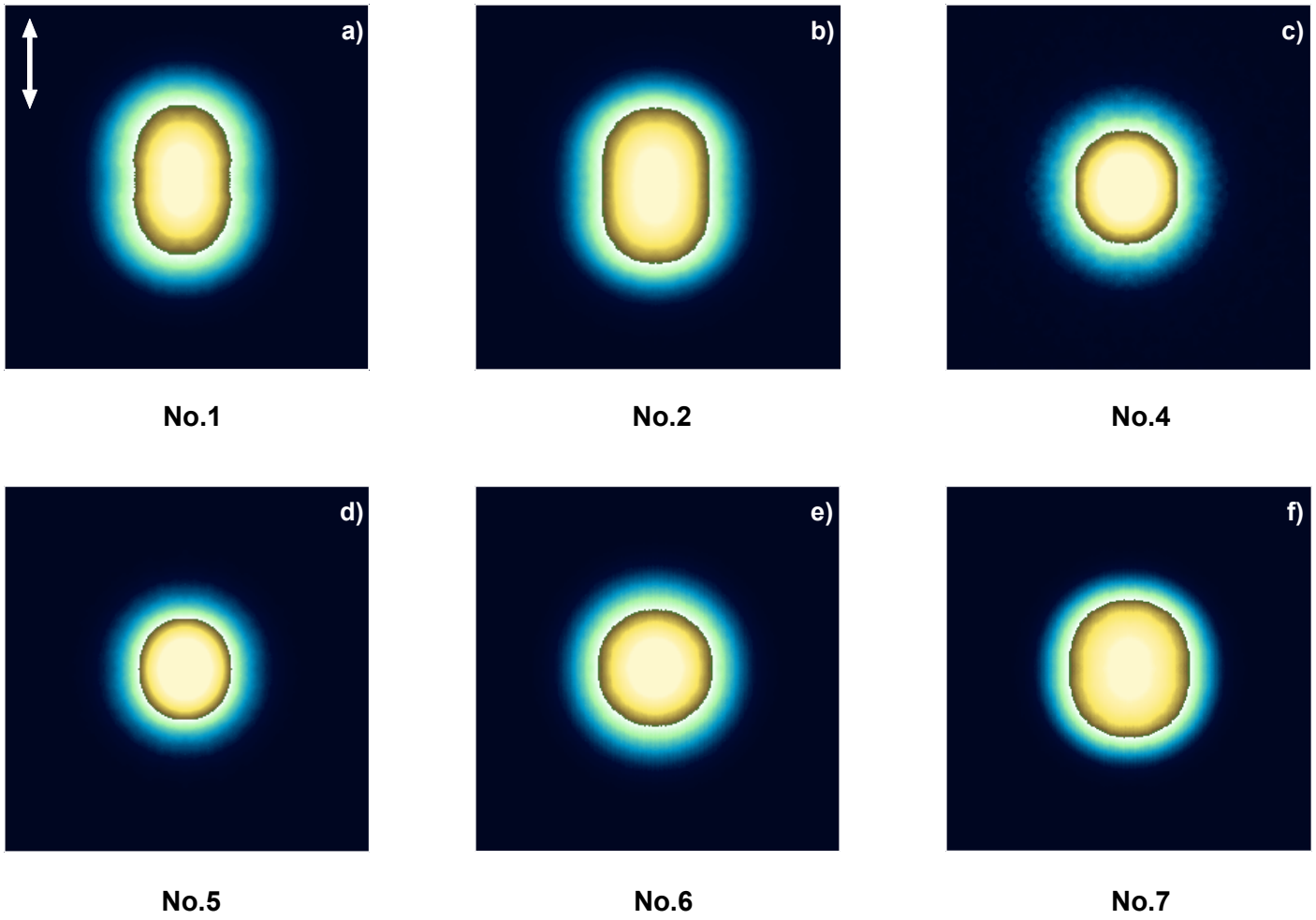

Fig. S10, C_2^+ ion images: Images recorded for the excitation no.1-2 and 4-7 as specified in **Table S1**. The laser polarization is indicated by a double arrow in (a).

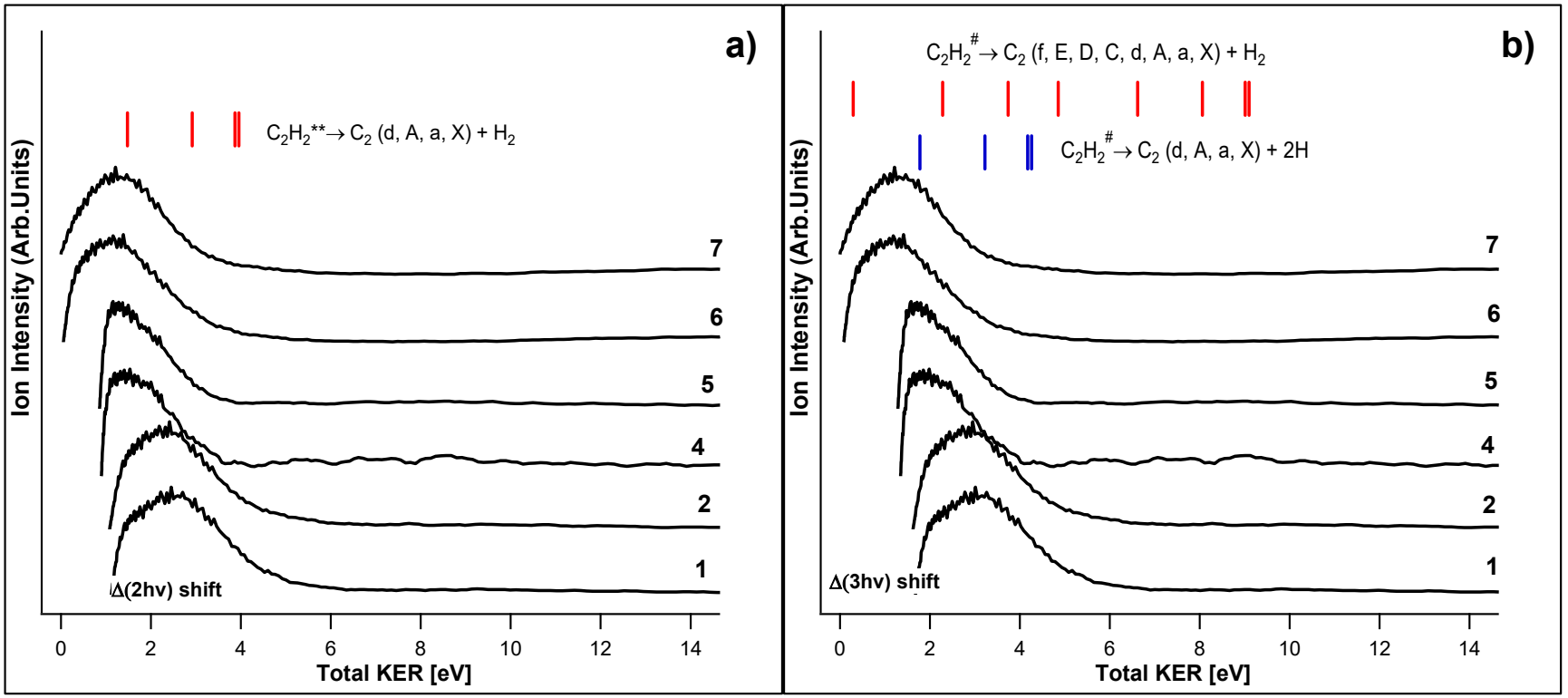

Fig. S11, C_2^+ kinetic energy release spectra (KERs): Ion kinetic energy release spectra (Ion-KERs) derived from the images no.1,2,4 -7 (see **Table S1**). The spectra are plotted as a function of the total kinetic energy release for the no. 7 (Total KER_0) and shifted by n-photon energy differences ($\Delta(n\mathit{hv})$) with respect to the "reference spectrum", no. 7 (see main text) as, $\Delta(\mathit{2hv})$ (a) and $\Delta(\mathit{3hv})$ (b). KER thresholds for fragment formations by n-photo-dissociation (n = 2 and 3 for photodissociation via the $C_2H_2^{**}$ and $C_2H_2^{\#}$ intermediate species; see main text), as specified, are indicated by sticks above the spectra.

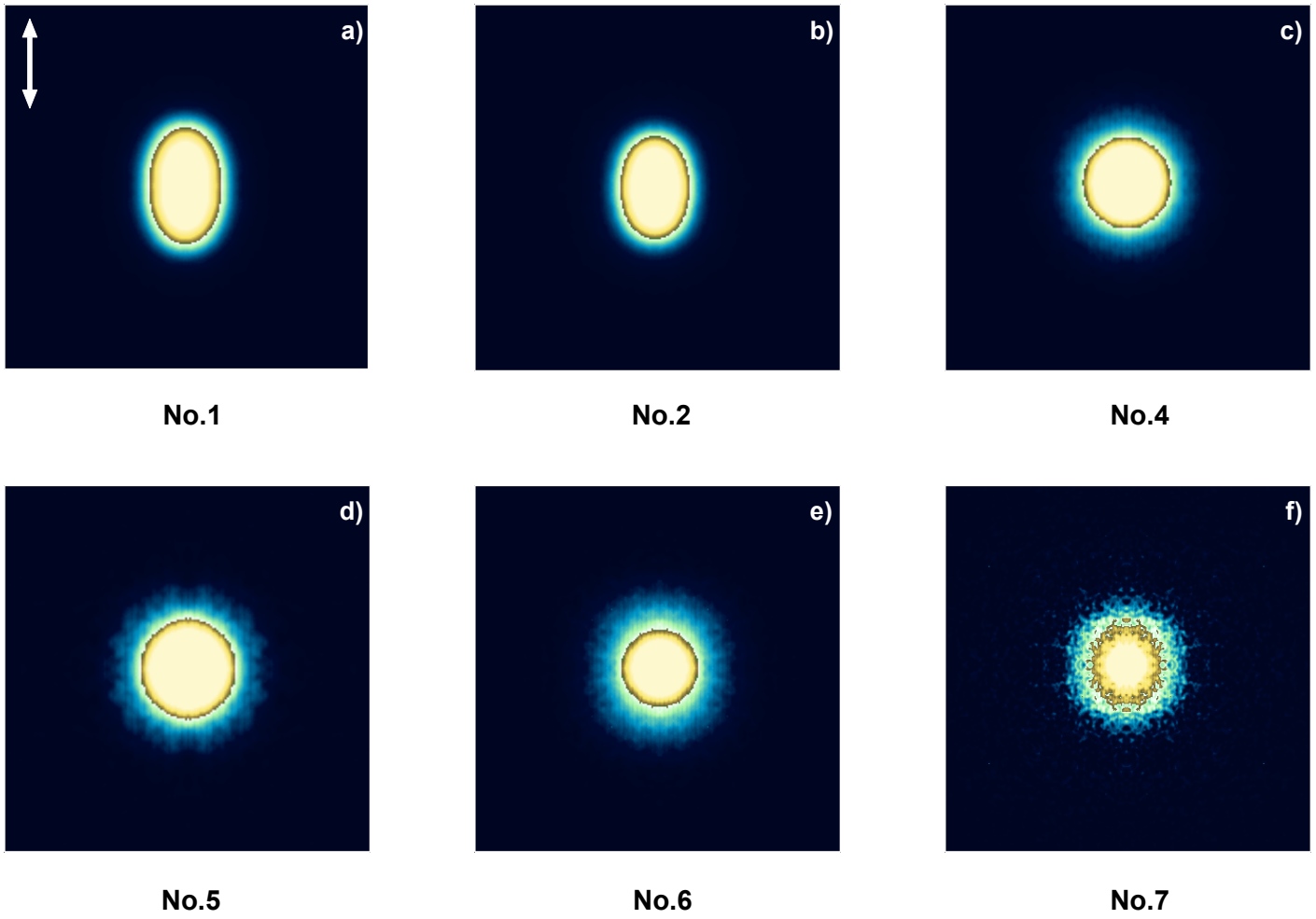

Fig. S12, C_2H^+ ion images: Images recorded for the excitation no.1-2 and 4-7 as specified in **Table S1**. The laser polarization is indicated by a double arrow in (a).

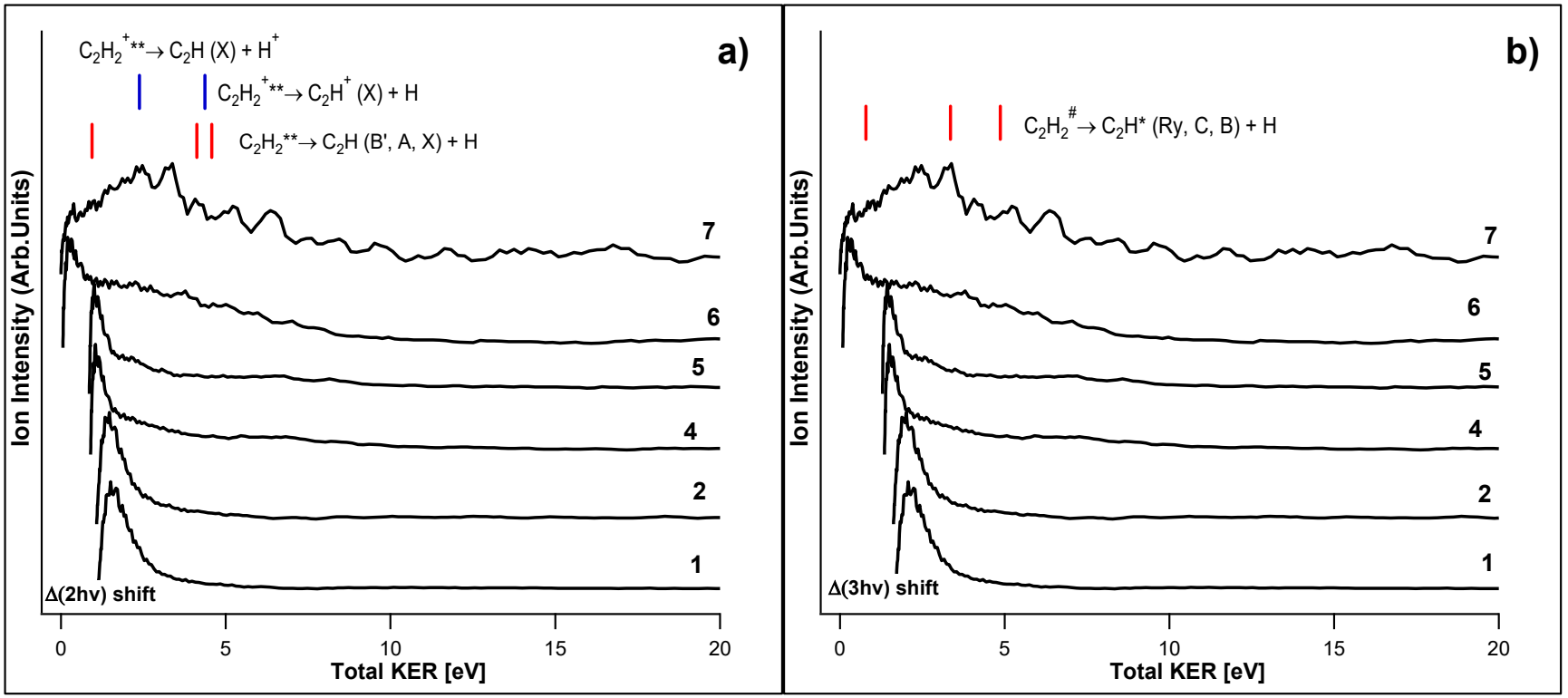

Fig. S13, C_2H^+ kinetic energy release spectra (KERs): Ion kinetic energy release spectra (Ion-KERs) derived from the images no.1,2,4 -7 (see **Table S1**). The spectra are plotted as a function of the total kinetic energy release for the no. 7 (Total KER_0) and shifted by n-photon energy differences (Δ(n*hv*)) with respect to the "reference spectrum", no. 7 (see main text) as, Δ(*2hv*) (a) and Δ(*3hv*) (b). KER thresholds for fragment formations by n-photo-dissociation (n = 2 and 3 for photodissociation via the C_2H_2** and $C_2H_2^{\#}$ intermediate species; see main text), as specified, are indicated by sticks above the spectra.

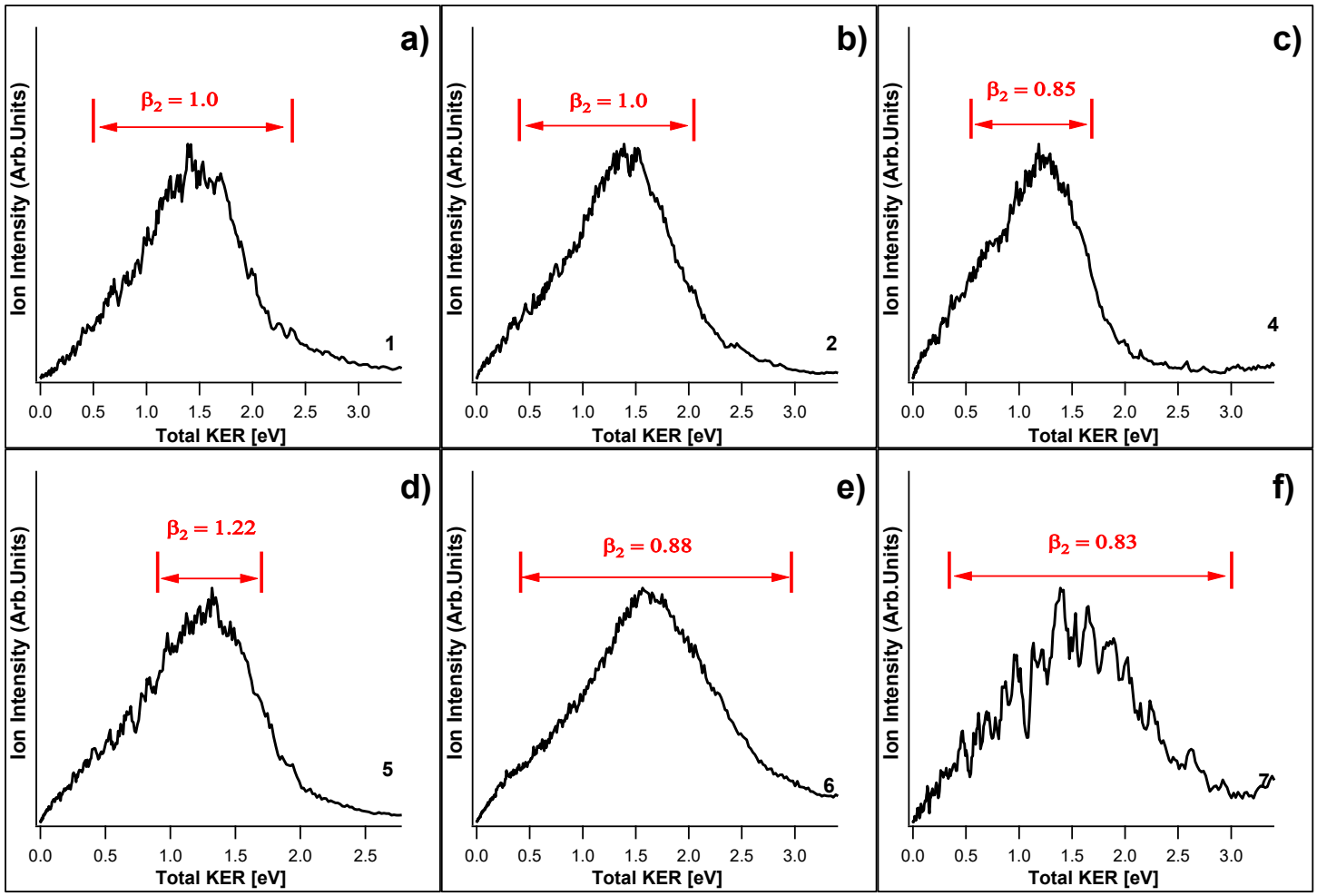

Fig. S14, H^+ angular distributions: H^+ KER spectra for images no. 1,2 and 4-7, average anisotropy / β_2 parameters (see **Table S2**) and energy ranges used for the β_2 determinations.

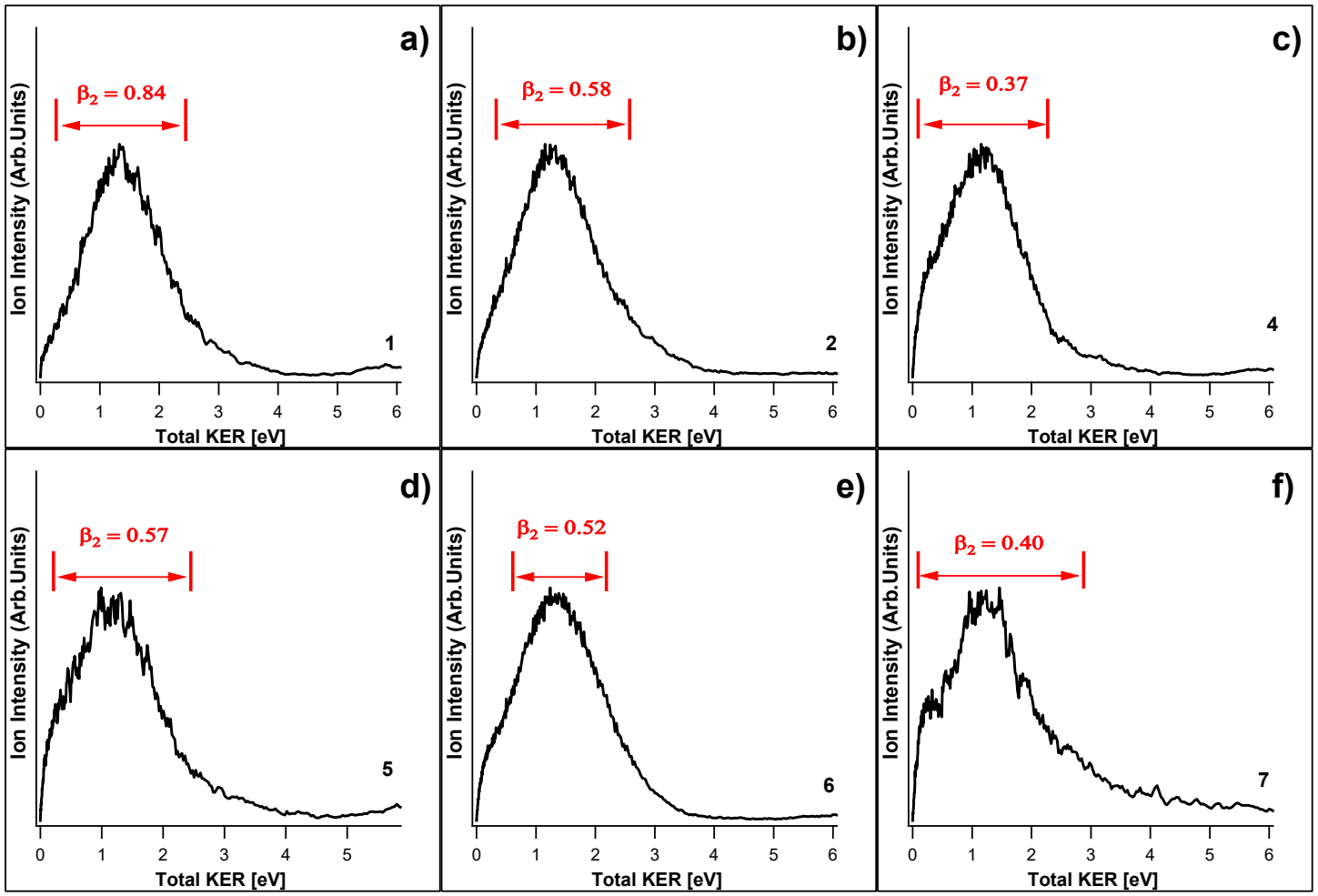

Fig. S15, C^+ angular distributions: C^+ KER spectra for images no. 1,2 and 4-7, average anisotropy / β_2 parameters (see **Table S2**) and energy ranges used for the β_2 determinations.

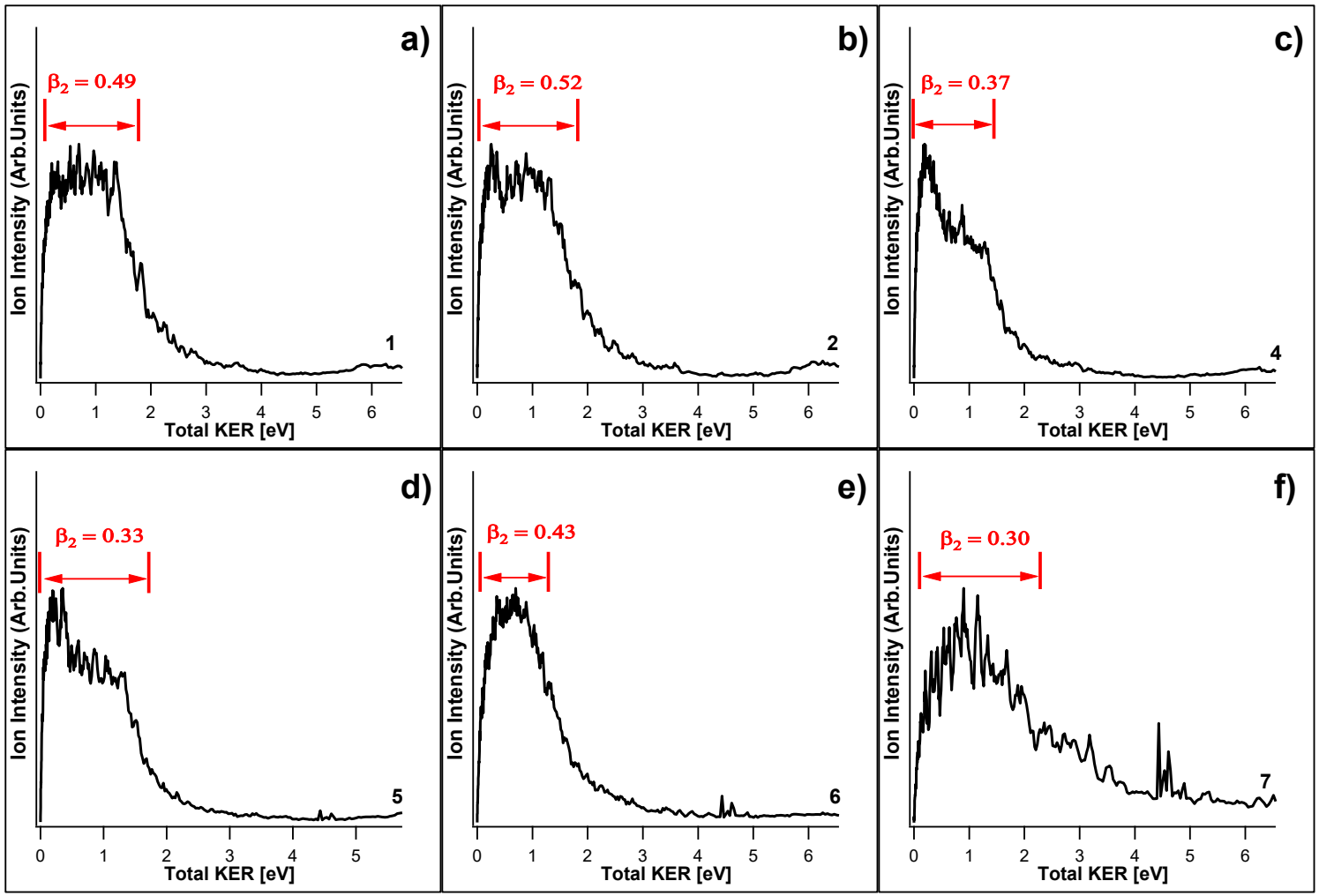

Fig. S16, CH^+ angular distributions: CH^+ KER spectra for images no. 1,2 and 4-7, average anisotropy / β_2 parameters (see **Table S2**) and energy ranges used for the β_2 determinations.

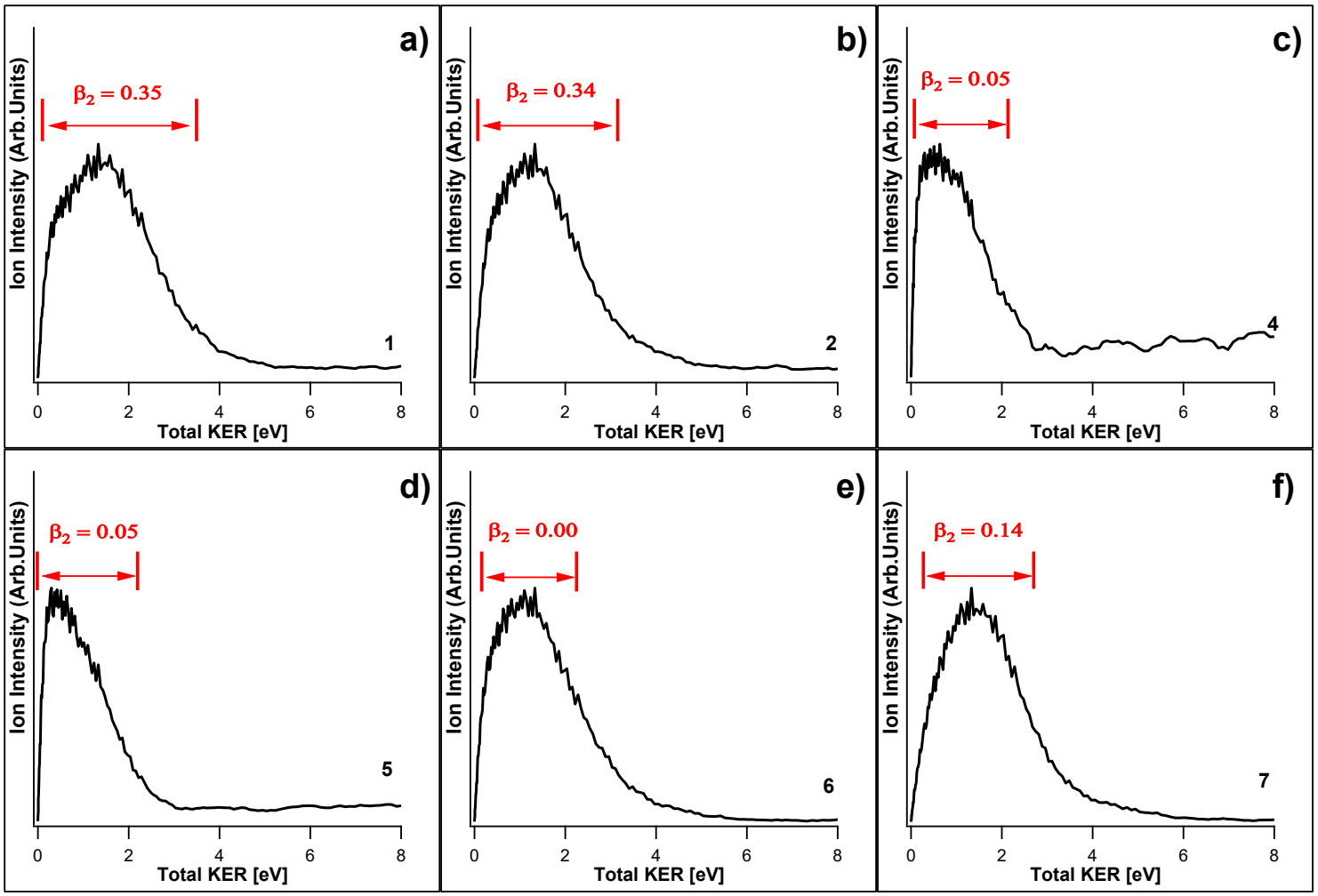

Fig. S17, C_2^+ angular distributions: C_2^+ KER spectra for images no. 1,2 and 4-7, average anisotropy / β_2 parameters (see **Table S2**) and energy ranges used for the β_2 determinations.

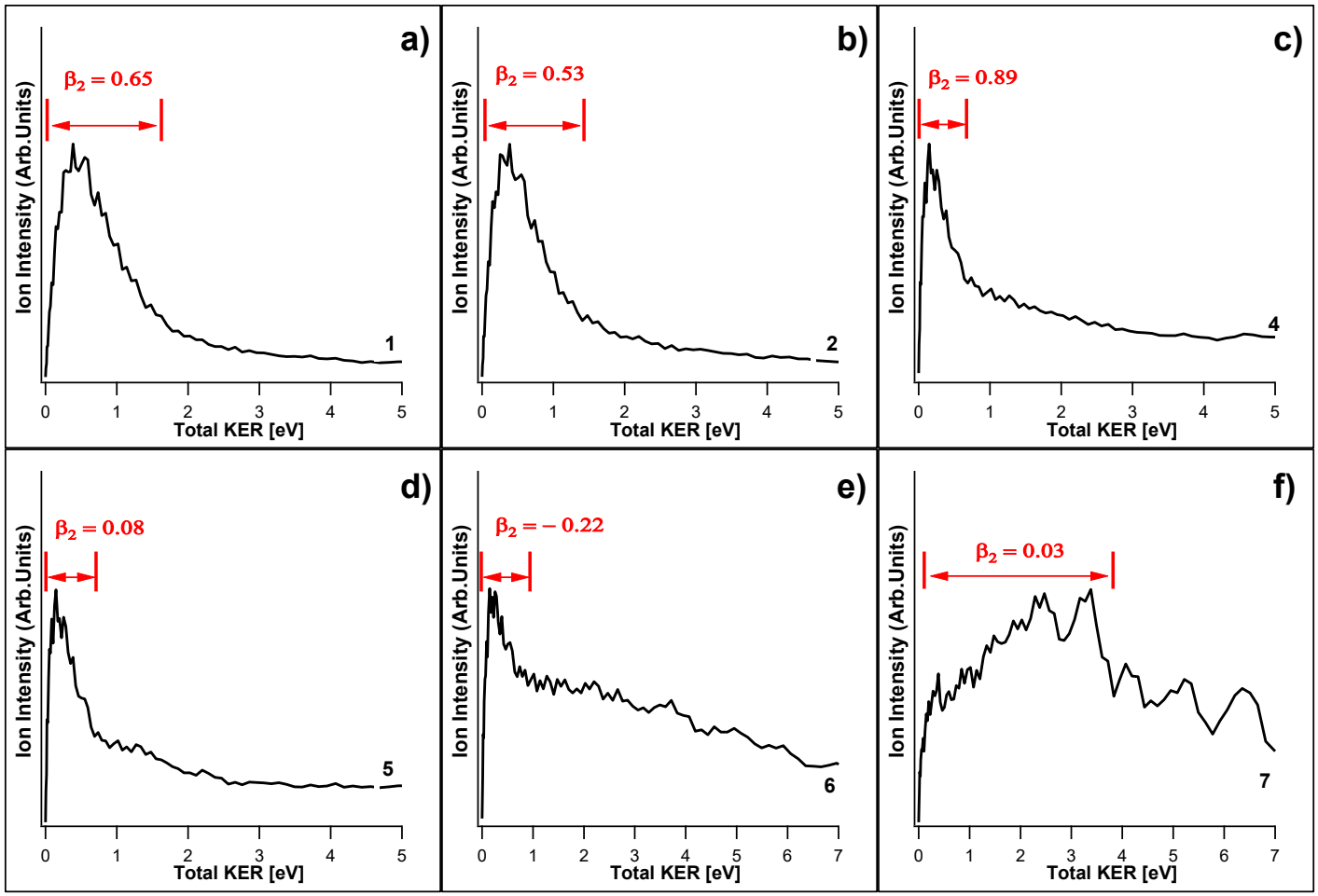

Fig. S18, C_2H^+ angular distributions: C_2H^+ KER spectra for images no. 1,2 and 4-7, average anisotropy / β_2 parameters (see **Table S2**) and energy ranges used for the β_2 determinations.

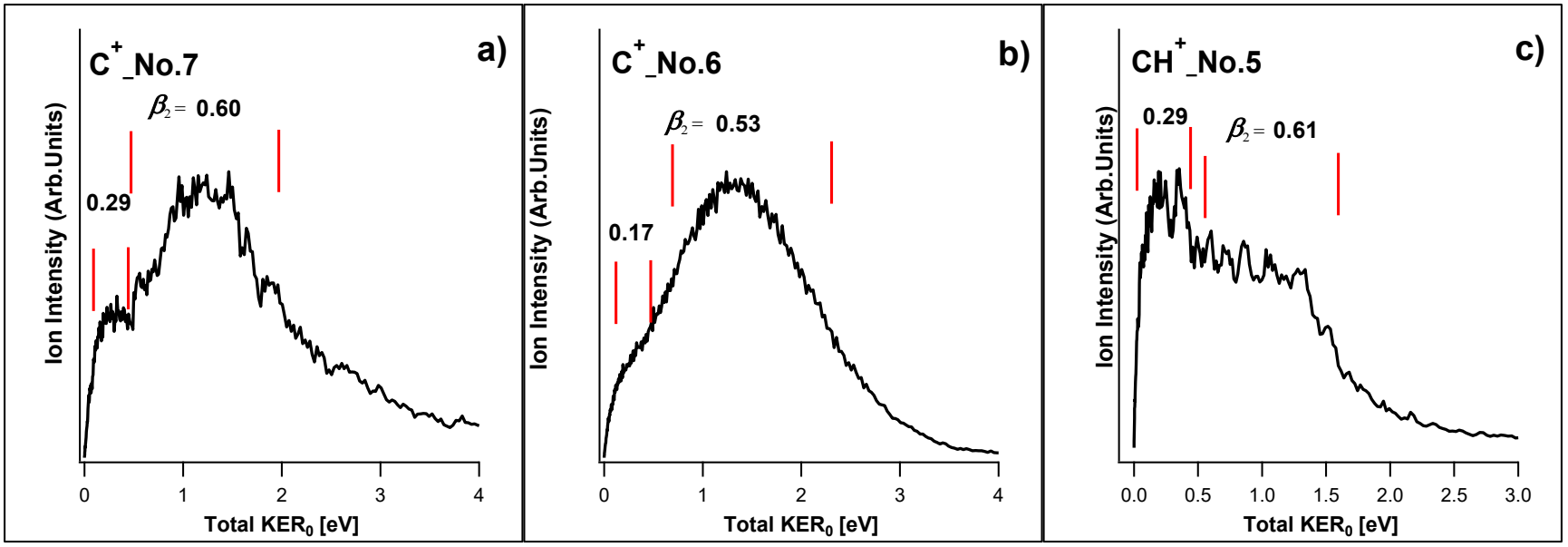

Fig. S19, Ion angular distributions: a) and b) C^+ KER spectra for images no. 7 and 6, **c)** CH^+ KER spectrum for image no.5 average anisotropy / β_2 parameters and energy ranges used for the β_2 determinations.

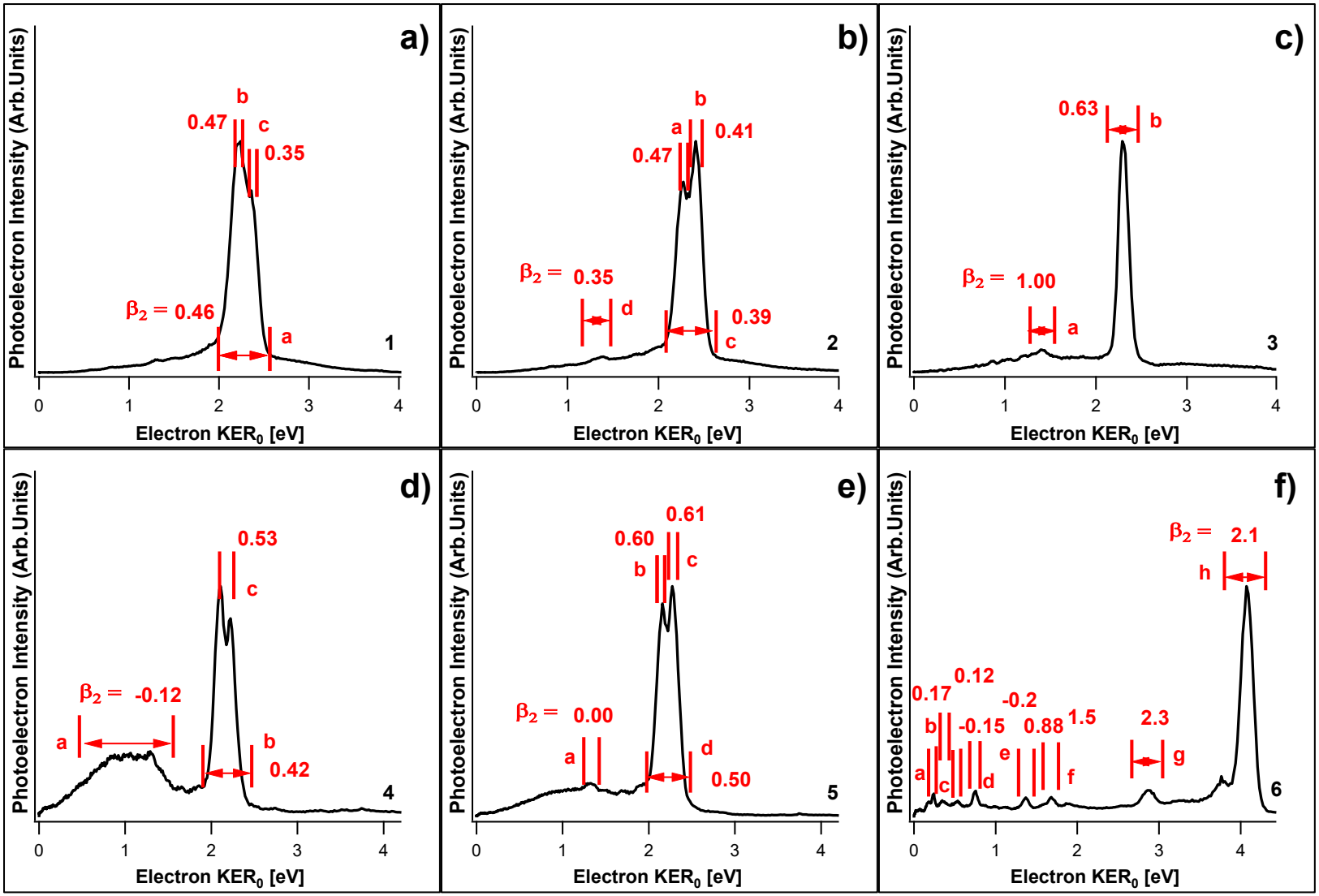
a)
b)
c)
d)
e)
f)
Photoelectron Intensity (Arb.Units)
Electron KER$_0$ [eV]
β_2 = 0.46
0.47
b
c
0.35
a
1
β_2 = 0.35
d
a
0.47
b
0.41
0.39
c
2
β_2 = 1.00
0.63
b
a
3
β_2 = -0.12
a
0.53
c
b
0.42
4
β_2 = 0.00
a
0.61
0.60
b
c
d
0.50
5
β_2 = 2.1
h
0.17
0.12
-0.2
b
-0.15
0.88
1.5
2.3
a
c
d
e
f
g
6

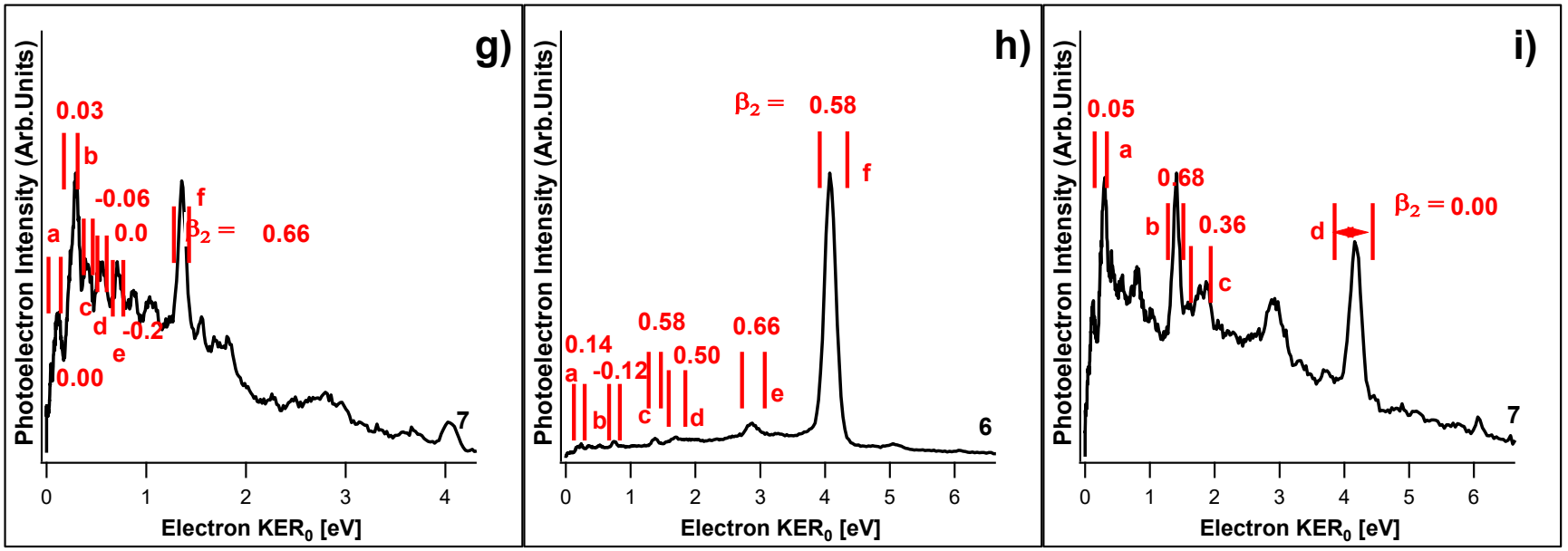

Fig. S20, photoelectron angular distributions: e-KER spectra for images no. 1-7, average anisotropy / β_2 parameters (see **Table S2**) and energy ranges used for the β_2 determinations. (f) and (h) recorded for repeller voltages of -3kV and -5kV, respectively for no.6 and (g) and (i) recorded for repeller voltages of -3kV and -5kV, respectively for no.7.

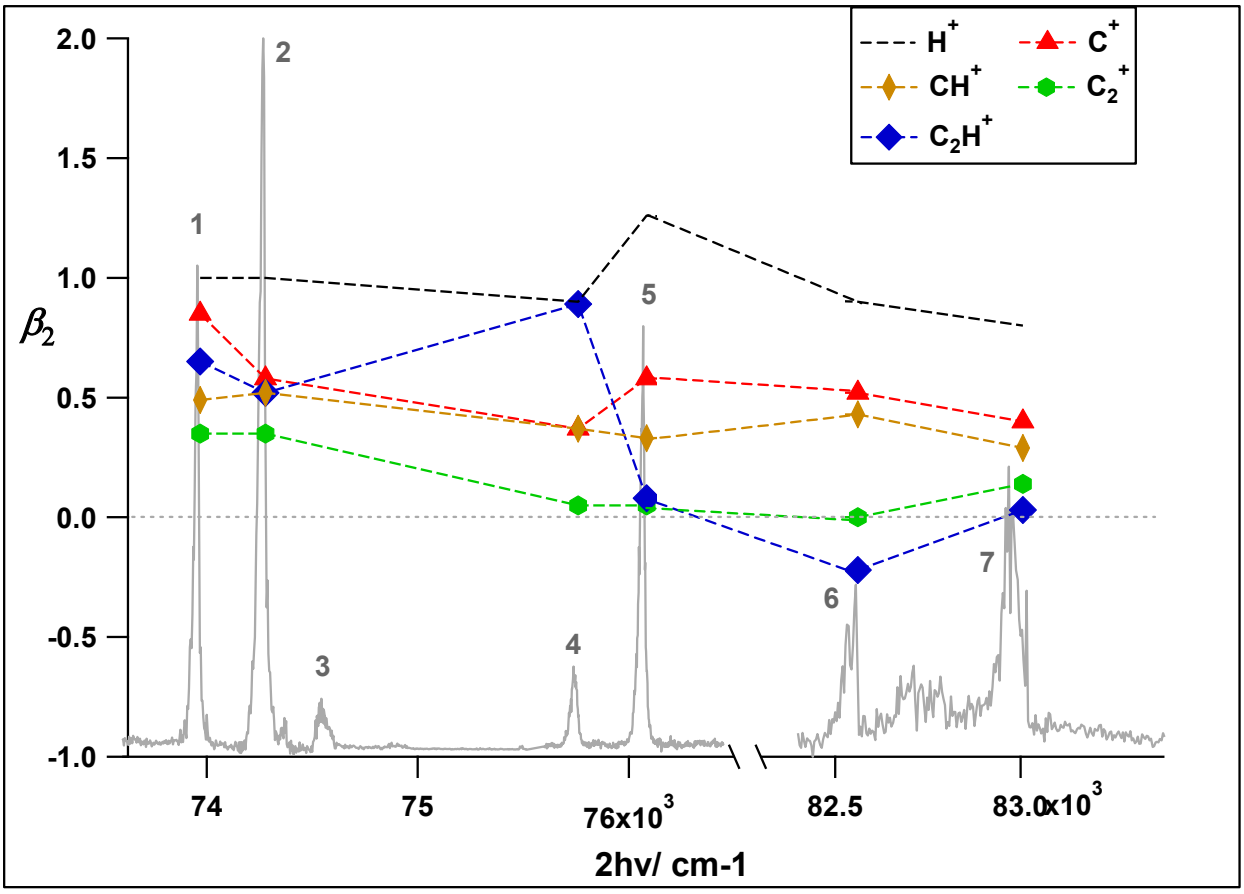

Fig. S21, β_2 parameters vs. ion images: Average β_2 parameters (**Table S2**) derived from ion images as a function of excitation**s (**no. 1,2, 4-7; **Table S1)** and ions.

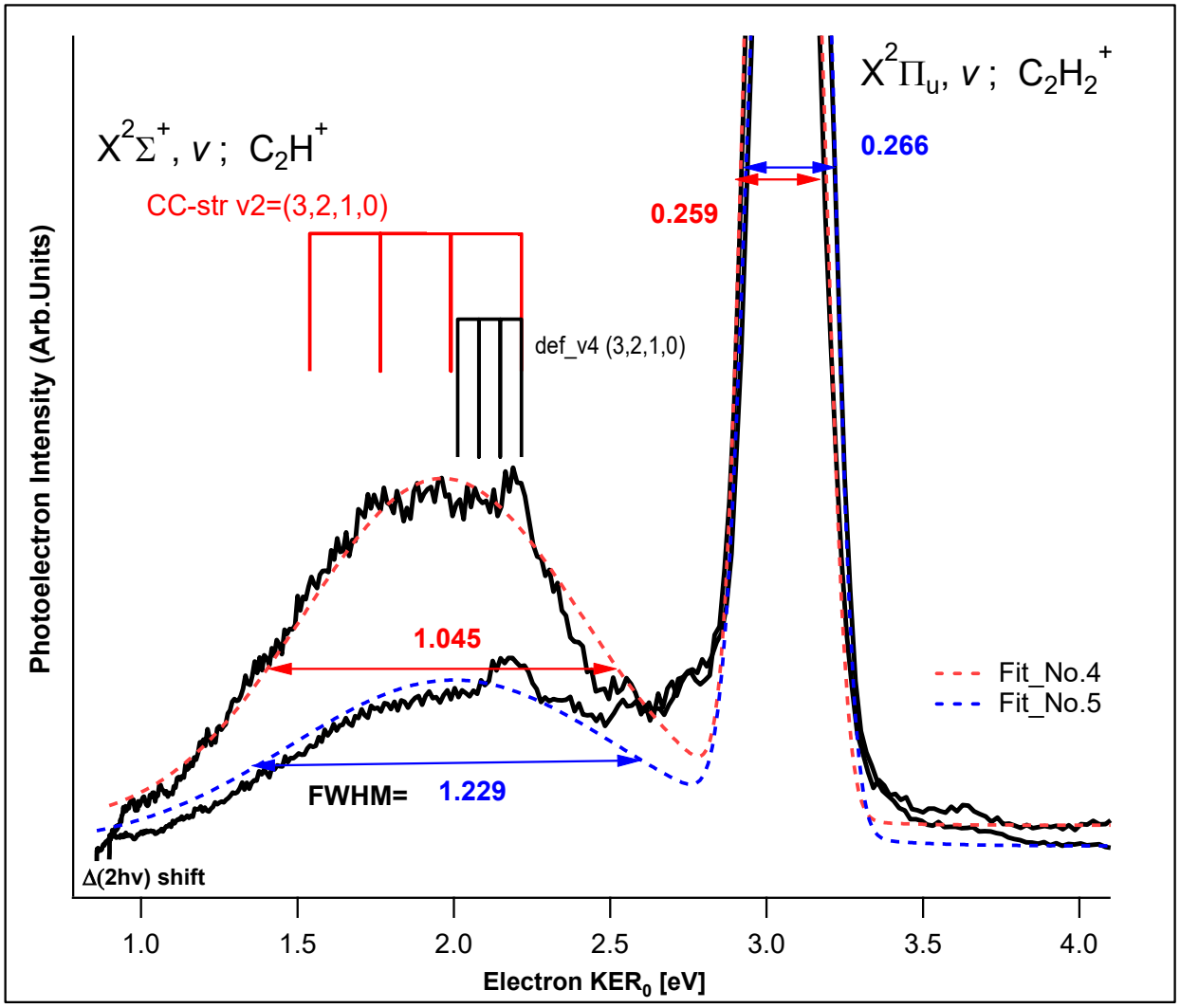

Fig. S22, electron KERs for images no. 4-5 (Table S1): e-KERs plotted as a function of the kinetic energy release (KER) for the no. 7 (KER_0), shifted by two-photon energy differences, ($\Delta(2h\nu)$) with respect to the "reference spectrum", no. 7 (see main text). Full width at half maximum (FWHM) of broad spectra were determined, as indicated. KER thresholds for $C_2H^+(X)$ vibrational mode formations, as specified, are indicated by sticks above the spectra.

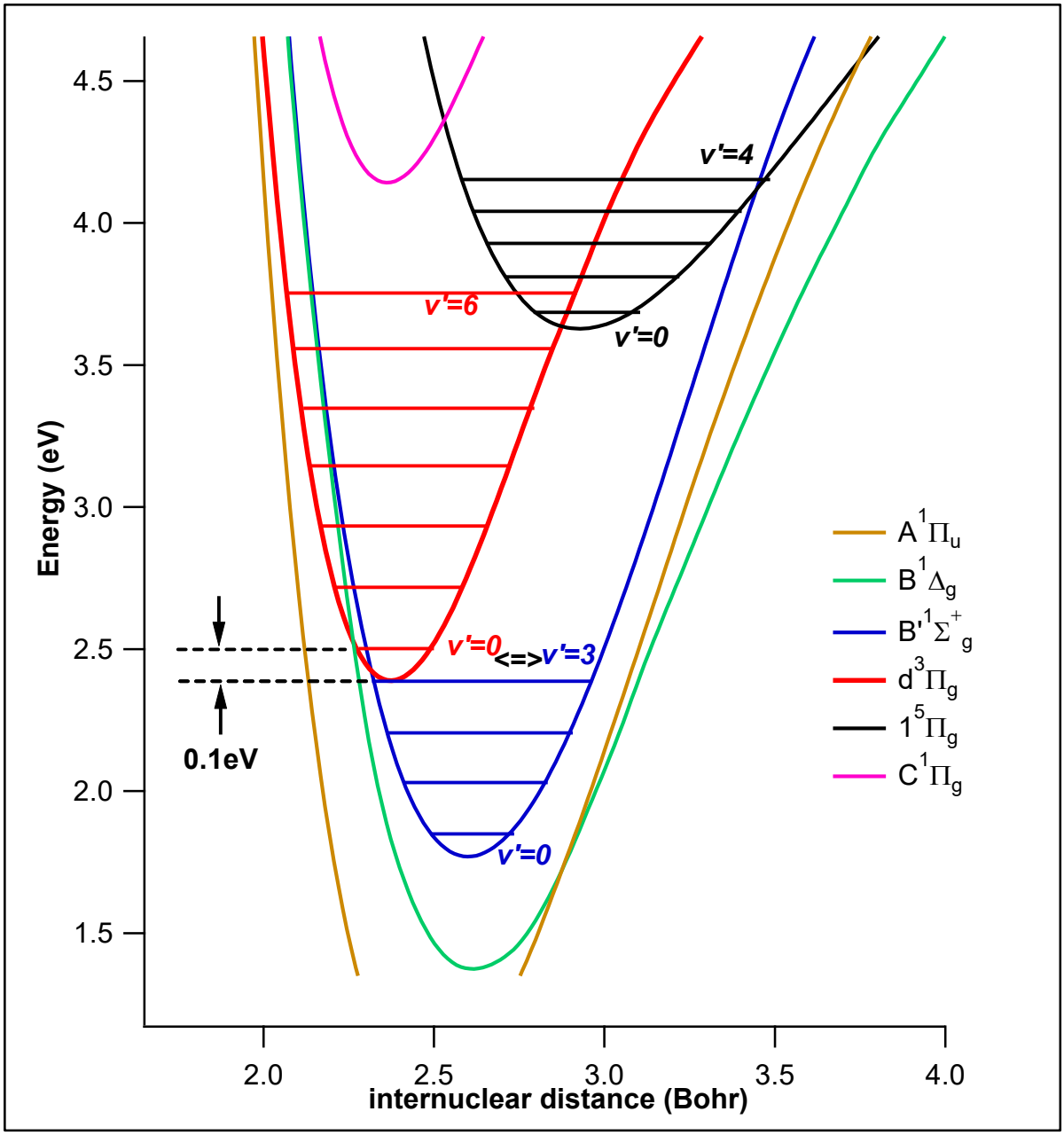

Fig. S23, Potential energy curves for excited C_2 states: Potential energy curves for C_2^{**} derived from ref. **[3]** and **[4]**). Spectroscopic constant for B′ $^1\Sigma_g^+$ state of ω_e=1424.11cm^{-1} and $\omega_e x_e$=2.57cm^{-1}were used.**[4]**

Tables S1, Images and resonant excitations.

Image no.	C_2H_2 Rydberg states; *nl*; $^1\Lambda_g$, $(v_1v_2v_3v_4v_5)$[a]	One-photon excitation/ nm	Two-photon excitation/ cm^{-1}
1	*3p*; $^1\Delta_g$, (00020)	270.364	73969
2	*3p*; $^1\Sigma_g$, (00000)	269.255	74279
3	*3p*; $^1\Sigma_g$, (01000)	268.262	74554
4	*3p*; $^1\Delta_g$, (01020)	263.992	75760
5	*3p*; $^1\Sigma_g$, (01000)	262.864	76085
6	*4p*; $^1\Delta_g$, (00000)	242.245	82561
7	*4p*; $^1\Sigma_g$, (00000)	240.947	83006

[a] n: principal quantum number for Rydberg electron. l: Rydberg electron orbital. (v_1, v_2, v_3, v_4, v_5): vibrational quantum numbers referring to vibrational modes. ν_1 (C-H symmetric stretch), ν_2 (C-C stretch) ν_3 (C-H asymmetric stretch), ν_4 and ν_5 (bend)

Table S2 (a), **Anisotropy parameters for images:** Anisotropy parameters, $\beta_n = \beta_2, \beta_4$, and β_6 determined from ion images (see **Fig. S14 – S18** for energy ranges) for n = 2 / 2,4 / 2,4,6 vs. ions and excitations (no/#, 1,2, 4 – 7; see **Table S1**).

#	Ion	β_2	β_4	β_6	Ion	β_2	β_4	β_6	Ion	β_2	β_4	β_6	Ion	β_2	β_4	β_6	Ion	β_2	β_4	β_6
1	**H^+**	0.87			**C^+**	0.78			**CH^+**	0.51			**C_2^+**	0.36			**CH_2^+**	0.71		
		1	-0.49			0.85	-0.2			0.49	0.06			0.35	0.02			0.65	0.18	
		1	-0.46	-0.14		0.85	-0.18	-0.03		0.49	0.06	-0.01		0.35	0	0.03		0.64	0.17	0.03
2		0.86				0.49				0.52				0.32				0.6		
		1	-0.55			0.58	-0.21			0.52	0.01			0.35	-0.06			0.52	0.18	
		1.01	-0.46	-0.33		0.59	-0.17	-0.08		0.51	-0.01	0.03		0.35	-0.05	-0.01		0.52	0.16	0.04
4		0.8				0.34				0.38				0.04				0.8		
		0.89	-0.37			0.37	-0.13			0.37	-0.06			0.05	-0.01			0.89	-0.37	
		0.89	-0.3	-0.27		0.37	-0.13	0.01		0.37	-0.05	-0.03		0.05	-0.01	-0.02		0.89	-0.3	-0.27
5		1.14				0.55				0.35				0.05				0.1		
		1.26	-0.46			0.58	-0.1			0.33	0.08			0.05	0.01			0.08	0.04	
		1.27	-0.38	-0.33		0.58	-0.1	-0.03		0.33	0.08	-0.01		0.05	0.01	0.02		0.07	0.01	0.05
6		0.84				0.51				0.42				0				-0.17		
		0.9	-0.21			0.52	-0.03			0.43	-0.02			0	-0.02			-0.22	0.12	
		0.9	-0.19	-0.1		0.53	0.01	-0.1		0.43	-0.02	-0.02		0	-0.01	-0.01		-0.22	0.13	-0.01
7		0.88				0.37				0.28				0.13				0.12		
		0.79	0.33			0.4	-0.12			0.29	0.05			0.14	-0.02			0.03	0.23	
		0.79	0.26	0.28		0.4	-0.1	-0.1		0.32	0.08	0.17		0.14	-0.03	0.02		0.01	0.16	0.18

Table S2 (b), **Anisotropy parameters for images: :** Anisotropy parameters, $\beta_n = \beta_2$ and β_4, determined from photoelectron images (see **Fig. S19 (a – g)** for energy ranges a - h) for n = 2 / 2,4 vs. excitations (no/#, 1 – 7; see **Table S1**). Repeller voltage: -3 kV.

-3kV		β_2	β_4	β_2	β_4	β_2	β_4	β_2	β_4	β_2	β_4	β_2	β_4	β_2	β_4	β_2	β_4
PES	**#**	**a**	**a**	**b**	**b**	**c**	**c**	**d**	**d**	**e**	**e**	**f**	**f**	**g**	**g**	**h**	**h**
	1	0.47		0.47		0.35											
		0.45	0.06	0.47	0.03	0.35	0.01										
	2	0.48		0.42		0.34		0.39									
		0.46	0.03	0.4	0.03	0.35	-0.03	0.38	0.02								
	3	1.29		0.71													
		0.82	1.16	0.55	0.37												
	4	-0.16		0.42		0.52											
		-0.07	-0.21	0.42	0.01	0.53	-0.03										
	5	-0.07		0.62		0.65		0.49									
		0.02	-0.19	0.57	0.07	0.57	0.06	0.5	-0.02								
	6	0.17		0.12		-0.16		-0.14		0.93		1.67		2.83		2.16	
		0.17	-0.01	0.12	-0.01	-0.14	-0.26	-0.35	-0.12	0.84	0.2	1.33	0.88	2.3	1.56	2.1	0.16
	7	0.01		0.05		-0.03		0.03		-0.23		0.61					
		-0.06	0.16	0.01	0.1	-0.11	0.16	-0.03	0.14	-0.18	-0.11	0.71	-0.3				

Table S2 (c), **Anisotropy parameters for images: :** Anisotropy parameters, $\beta_n = \beta_2$ and β_4, determined from photoelectron images (see **Fig. S19 (h – i)** for energy ranges, a - f) for n = 2 / 2,4 vs. excitations (no. / #: 6 – 7; see **Table S1**). Repeller voltage: -5 kV.

-5kV		β_2	β_4	β_2	β_4	β_2	β_4	β_2	β_4	β_2	β_4	β_2	β_4
PES	**#**	**a**	**a**	**b**	**b**	**c**	**c**	**d**	**d**	**e**	**e**	**f**	**f**
	6	0.13		-0.14		0.56		0.5		0.72		0.56	
		0.14	-0.01	-0.09	-0.11	0.6	-0.09	0.5	-0.01	0.6	0.3	0.6	-0.1
	7	0.06		0.67		0.39		0.13					
		0.04	0.04	0.69	-0.03	0.33	0.12	-0.03	0.35				

Table S3, Dissociation products: Low-lying valance states of CH/CH*, correlating to H (n=1) + C ($^3P_0$, $^1D_2$, $^1S_0$, $^5S^o_2$),according to *ab initio* calculation by Vázquez et al.[5]

Molecular states	Atomic energies (eV)	Atomic states
$c^4\Sigma^-$, $(1)^6\Sigma^-$	*4.182*	C($^5S^o_2$)
$(2)^2\Sigma^+$,	*2.684*	C($^1S_0$)
$A^2\Delta$,$C^2\Sigma^+$, $(2)D^2\Pi$	*1.263*	C($^1D_2$)
$X^2\Pi$, $B^2\Sigma^-$, $a^4\Sigma^-$, $b^4\Pi$	*0.000*	C($^3P_0$)

Table S4 (a) Thresholds vs. fragment dissociation: Dissociaction energies (D_0) for fragments of C_2H_2. m(min) are the minimum number of photons required for the fragment formations in multiphoton dissociation, corresponding to excitation no. 7 (**Table S1**).

Fragment	D_0(eV)	m(min)/*hv*
H(n=1) + C_2H(X)	5.712[a]	2
H*(n=2) + C_2H(X)	15.911[b]	4
H(n=1) + C_2H*(B')	9.352[b]	2
H2 + C_2(X)	6.333[c]	2
H2 + C_2(d)	8.816[b]	2
H2 + C_2(C)	10.581[b]	3
CH_2(X)+ C($^3P_0$)	9.170[c]	2
CH_2(X)+ C*($^1D_2$)	10.433[b]	3
CH_2(X)+ C*($^1S_0$)	11.854[b]	3
CH_2(X)+ C*($^5S^o_2$)	13.352[b]	3
CH_2(X)+ C*($^3P^o_0$)	16.650[b]	4
CH_2(X)+ C*($^1P^o_1$)	16.854[b]	4
CH_2(X)+ C*($^3D^o_3$)	17.115[b]	4
CH(X)+ CH(X)	9.921[d]	2
CH(X)+ CH*(A)	12.796[b]	3
CH(X)+ CH*(B)	13.150[b]	3
CH(X)+ CH*(C)	13.864[b]	3
2H + C_2(X)	11.174[b]	3
2H + C_2*(d)	13.657[b]	3
2H + C_2*(C)	15.422[b]	4
CH(X)+H+ C($^3P_0$)	13.666[b]	3
H_2+ C($^3P_0$) +C($^3P_0$)	12.475[b]	3

a. From Mordaunt's paper (Ref. [6])
b. Calculated values refers to fragment energetic in NIST (Ref. [7])
c. From Matthíasson's paper (Ref. [8])
d. From Evrin's paper (Ref. [9])

Table S4 (b), Thresholds vs. ionizations: Ionization energies (IE) for the parent molecule and fragments. m(min) are the minimum number of photons required for ionization of the species in multiphoton excitation, corresponding to excitation no. 7 (**Table S1**). E_{thr} are common thresholds for ionization of fragment species according to equation $E_{thr}(Fi/Fi^*) = nh\nu - IE(Fi/Fi^*)$; n = 1,2,3 with respect to the "reference spectrum", no. 7. (see main text).

Molecule	m(min) / *hv*	IE(eV)	E_{thr}(eV)
$C_2H_2(X)$	3	11.400	4.037
Fragments	m(min) / *hv*	IE(eV)	E_{thr}(eV)
H(n=1)	3	13.598	1.837
H*(n=2)	1	13.598	1.744
$C(^3P_0)$	3	11.260	4.177
$C^*(^1D_2)$	2	11.260	0.295
$C^*(^1S_0)$	2	11.260	1.715
$C^*(^5S^o_2)$	2	11.260	3.214
$C^*(^3P^o_0)$	1	11.260	1.366
$C^*(^1P^o_1)$	1	11.260	1.570
$C^*(^3D^o_3)$	1	11.260	1.831
CH(X)	3	10.640	4.797
CH*(A)	2	10.640	2.521
CH*(B)	2	10.640	2.882
CH*(C)	2	10.640	3.595
$CH_2(X)$	3	10.640	5.037
$C_2(X)$	3	11.866	3.659
C_2*(d)	2	11.866	0.908
C_2*(C)	2	11.866	2.450
$C_2H(X)$	3	11.610	3.827
$C_2H^*(B')$	2	11.610	2.321

a. From NIST (Ref. [7])
b. From Krechkivska's paper (Ref. [10])

References:

1. M. N. R. Ashfold, B. Tutcher, B. Yang, Z. K. Jin and S. L. Anderson, *J. Chem. Phys.*, 1987, **87**, 5105-5115.
2. K. Tsuji, N. Arakawa, A. Kawai and K. Shibuya, *J. Phys. Chem. A*, 2002, **106**, 747-753.
3. J. F. Babb, R. T. Smyth and B. M. McLaughlin, *Astrophys. J*, 2019, **876**, 38.
4. M. Martin, *J. Photochem. Photobiol. A*, 1992, **66**, 263-289.
5. G. J. Vázquez, J. M. Amero, H. P. Liebermann, R. J. Buenker and H. Lefebvre-Brion, *J. Chem. Phys.*, 2007, **126**, 164302.
6. D. H. Mordaunt and M. N. R. Ashfold, *J. Chem. Phys.*, 1994, **101**, 2630-2631.
7. NIST Chemistry WebBook - (National Institute of Standards and Technology) https://webbook.nist.gov/chemistry/name-ser/
8. K. Matthíasson, H. Wang and Á. Kvaran, *Chem.Phys. L*, 2008, **458**, 58-63.
9. K. M. Ervin, S. Gronert, S. E. Barlow, M. K. Gilles, A. G. Harrison, V. M. Bierbaum, C. H. DePuy, W. C. Lineberger and G. B. Ellison, *J. Am. Chem. Soc.* , 1990, **112**, 5750-5759.
10. O. Krechkivska, G. B. Bacskay, B. A. Welsh, K. Nauta, S. H. Kable, J. F. Stanton and T. W. Schmidt, *J. Chem. Phys.*, 2016, **144**, 144305.